JNeurosci
THE JOURNAL OF NEUROSCIENCE

Research Articles: Behavioral/Cognitive

Concurrent- and after-effects of medial temporal lobe stimulation on directed information flow to and from prefrontal and parietal cortices during memory formation

https://doi.org/10.1523/JNEUROSCI.1728-22.2023

Cite as: J. Neurosci 2023; 10.1523/JNEUROSCI.1728-22.2023

Received: 10 September 2022
Revised: 6 March 2023
Accepted: 13 March 2023

Concurrent- and after-effects of medial temporal lobe stimulation on directed information flow to and from prefrontal and parietal cortices during memory formation

Anup Das[1] *and Vinod Menon*[1,2,3]

Department of Psychiatry & Behavioral Sciences[1]
Department of Neurology & Neurological Sciences[2]
Stanford Neurosciences Institute[3]
Stanford University School of Medicine
Stanford, CA 94305

Title: Concurrent- and after-effects of medial temporal lobe stimulation on directed information flow to and from prefrontal and parietal cortices during memory formation

Abbreviated title: Stimulation effects on cortical information flow

Author names and affiliations, including postal codes:

Anup Das, Department of Psychiatry & Behavioral Sciences, Stanford University School of Medicine, Stanford, CA 94305

Vinod Menon, Department of Psychiatry & Behavioral Sciences, Department of Neurology & Neurological Sciences, and Stanford Neurosciences Institute, Stanford University School of Medicine, Stanford, CA 94305

Corresponding author email address: a1das@stanford.edu, menon@stanford.edu

Number of pages: 64

Number of figures: 7

Number of tables: 6

Number of words in Abstract: 250

Number of words in Introduction: 1543

Number of words in Discussion: 2758

Conflict of interest statement: The authors declare no competing financial interests.

Acknowledgements

This research was supported by NIH grants NS086085 and EB022907. We thank Dr. Yuan Zhang for assistance with statistical analysis.

Abstract

Electrical stimulation of the medial temporal lobe (MTL) has the potential to uncover causal circuit mechanisms underlying memory function. However, little is known about how MTL stimulation alters information flow with frontoparietal cortical regions implicated in episodic memory. We used intracranial electroencephalography recordings from humans (14 participants, 10 females) to investigate how MTL stimulation alters directed information flow between MTL and prefrontal cortex (PFC) and between MTL and posterior parietal cortex (PPC). Participants performed a verbal episodic memory task during which they were presented with words and asked to recall them after a delay of ~20 seconds. 50 Hz stimulation was applied to MTL electrodes on selected trials during memory encoding. Directed information flow was examined using phase transfer entropy. Behaviorally, we observed that MTL stimulation reduced memory recall. MTL stimulation decreased top-down PFC→MTL directed information flow during both memory encoding and subsequent memory recall, revealing aftereffects more than 20 seconds after end of stimulation. Stimulation suppressed top-down PFC→MTL influences to a greater extent than PPC→MTL. Finally, MTL→PFC information flow on stimulation trials was significantly lower for successful, compared to unsuccessful, memory recall; in contrast, MTL→ventral PPC information flow was higher for successful, compared to unsuccessful, memory recall. Together these results demonstrate that the effects of MTL stimulation are behaviorally, regionally, and directionally specific, that MTL stimulation selectively impairs directional signaling with PFC, and that causal MTL-ventral PPC circuits support successful memory recall. Findings provide new insights into dynamic casual circuits underling episodic memory and their modulation by MTL stimulation.

Significance Statement

The medial temporal lobe (MTL) and its interactions with prefrontal cortex (PFC) play a critical role in human memory. Dysfunctional MTL-PFC circuits are prominent in psychiatric and neurological disorders including Alzheimer's disease and schizophrenia. Brain stimulation has emerged as a potential mechanism for enhancing memory and cognitive functions, but the underlying neurophysiological mechanisms and dynamic causal circuitry underlying bottom-up and top-down signaling involving the MTL are unknown. Here, we use intracranial electroencephalography recordings to investigate the effects of MTL stimulation on causal signaling in key episodic memory circuits linking the MTL with PFC. Our findings have implications for translational applications aimed at realizing the promise of brain stimulation-based treatment of memory disorders.

Introduction

The medial temporal lobe (MTL) and its interactions with prefrontal cortex (PFC) play a foundational role in human memory (Amer & Davachi, 2022; Cabeza, Ciaramelli, Olson, & Moscovitch, 2008; Curtis, 2006; Eichenbaum, 2017; Husain & Nachev, 2007; Rolls, 2018, 2019; Rutishauser, Reddy, Mormann, & Sarnthein, 2021; Vogt & Pandya, 1987; Wagner, Shannon, Kahn, & Buckner, 2005). Dysfunctional MTL-PFC circuits are prominent in psychiatric and neurological disorders including Alzheimer's disease and schizophrenia (Dickerson & Eichenbaum, 2010; Meyer-Lindenberg et al., 2005; Uhlhaas & Singer, 2012). Brain stimulation has emerged as a potential mechanism for enhancing memory function (Alagapan, Lustenberger, Hadar, Shin, & Fröhlich, 2019; Ezzyat et al., 2018; Fell et al., 2013; Kucewicz, Berry, Miller, et al., 2018; van der Plas, Braun, Stauch, & Hanslmayr, 2021; J. X. Wang et al., 2014; Yeh & Rose, 2019) and cognitive function (Grover, Nguyen, & Reinhart, 2021; Ramirez-Zamora et al., 2020), but the underlying neurophysiological mechanisms and dynamic causal circuitry underlying bottom-up and top-down signaling involving the MTL are poorly understood. Given its critical role in memory formation, deep brain stimulation of the MTL with simultaneous recordings in the MTL and PFC has the potential to inform causal circuit mechanisms of encoding and recall in the human brain. Here, we use intracranial electroencephalography (iEEG) recordings to investigate the effects of MTL stimulation on causal signaling in key episodic memory circuits linking the MTL with PFC.

Electrophysiological studies in rodents have reported greater information flow from the MTL to the medial PFC than the reverse during spatial working memory (Zhang, Guo, & Liu, 2022). In non-human primates, MTL-dorsolateral and -ventrolateral PFC interactions have been linked

with memory performance (Brincat & Miller, 2015; Cruzado, Tiganj, Brincat, Miller, & Howard, 2020). In humans, fMRI studies have consistently found coactivation of the MTL and multiple PFC regions during both spatial and verbal memory tasks (Dickerson & Eichenbaum, 2010; Dobbins, Foley, Schacter, & Wagner, 2002; M. Moscovitch, Cabeza, Winocur, & Nadel, 2016; Qin et al., 2014; Rugg & Vilberg, 2013; Simons & Spiers, 2003). Moreover, MTL-ventromedial PFC coactivation is also associated with better memory performance (Kumaran, Summerfield, Hassabis, & Maguire, 2009). Other studies have shown that functional connectivity between the MTL and medial PFC is also associated with memory recall (Preston & Eichenbaum, 2013; Qin et al., 2014; van Kesteren, Fernández, Norris, & Hermans, 2010). Furthermore, non-invasive magnetoencephalography studies in humans have suggested that coherence between the MTL and the superior frontal gyrus and medial PFC subdivisions in the delta-theta frequency band is associated with successful memory integration (Backus, Schoffelen, Szebényi, Hanslmayr, & Doeller, 2016; Guitart-Masip et al., 2013; Spaak & de Lange, 2020). iEEG studies in humans have reported increased MTL-dorsolateral and -ventrolateral PFC theta band synchronization during episodic memory encoding and recall compared to resting baseline conditions (Anderson, Rajagovindan, Ghacibeh, Meador, & Ding, 2010; Das & Menon, 2021; Ekstrom & Watrous, 2014; Watrous, Tandon, Conner, Pieters, & Ekstrom, 2013).

Although prior non-invasive studies have provided significant insights into the role of the MTL and PFC in human episodic memory processing, the causal effects of brain stimulation on the electrophysiology of dynamic “bottom-up” and “top-down” interactions involving the PFC remains unknown. While non-invasive transcranial magnetic stimulation can be used to transiently alter neural processing in targeted cortical regions (J. X. Wang et al., 2014; Yeh &

Rose, 2019), it cannot precisely target deep brain structures such as the MTL (Kim, Ekstrom, & Tandon, 2016; Rossini & Rossi, 2007). Intracranial electrical stimulation provides an alternative approach that can more precisely map functional brain circuits (Mohan et al., 2020; Paulk et al., 2022) and assess the neurophysiological basis of cognitive processes and its causal basis (Grover et al., 2021; Huang & Keller, 2022; Mercier et al., 2022).

We recently found evidence for asymmetric frequency-specific feedforward and feedback information flow between hippocampus and PFC during memory formation (Das & Menon, 2021). Specifically, we found higher directed information flow from the MTL to the PFC than the reverse, in delta-theta frequency band and higher directed information flow from the PFC to the MTL, than the reverse, in the beta frequency band (Das & Menon, 2021, 2022). Crucially, these findings were observed during both memory encoding and recall periods, indicating a prominent role of delta-theta for "bottom-up" signaling and beta for "top-down" signaling in the cortex.

Here we use iEEG data from the UPENN-RAM consortium (Goyal et al., 2018; Jacobs et al., 2016) to investigate how MTL stimulation alters directed information flow between the MTL and the PFC during episodic memory processing. Participants were presented a list of words during the encoding period and after a short delay, were asked to recall as many words as possible from the list. During encoding, stimulation was applied at 50 Hz to select MTL electrodes on alternate word pairs, and memory recall was probed after a ~20 second delay period. The choice of 50 Hz stimulation frequency was motivated by its overlap with the gamma band (30-80 Hz) which has been associated with human episodic memory and the amplitude of

iEEG fluctuations in this frequency band has been shown to reflect the underlying activity of single-neurons (Kahana, 2006; Kucewicz et al., 2014; Lachaux, Axmacher, Mormann, Halgren, & Crone, 2012). Moreover, previous studies have reported that MTL stimulation applied in the 40-50 Hz range has a direct impact on memory performance (Fell et al., 2013; Inman et al., 2018; Suthana et al., 2012). We investigated how MTL stimulation alters its information flow with the PFC. We used phase transfer entropy (PTE) (Hillebrand et al., 2016; Lobier, Siebenhühner, Palva, & Matias, 2014; M. Y. Wang et al., 2017) which provides a robust and powerful measure for characterizing information flow between brain regions based on phase coupling and, crucially, it captures linear as well as nonlinear intermittent and nonstationary dynamics in iEEG data (Hillebrand et al., 2016; Lobier et al., 2014; Menon et al., 1996).

The main goal of our study was to investigate how MTL stimulation alters directed information flow between the MTL and the PFC. We build on our recent findings of asymmetric frequency-dependent directed information flow focused on the delta-theta (0.5-8 Hz) and beta (12-30 Hz) frequency bands (Das & Menon, 2021, 2022). Our analysis focused on the middle frontal gyrus (MFG) encompassing the dorsolateral PFC regions implicated in memory formation and monitoring (Chua & Ahmed, 2016; Rugg, 2022). We contrast this with MTL interactions with the inferior frontal gyrus (IFG) encompassing the ventrolateral PFC regions which has been implicated in controlled retrieval (Badre, Poldrack, Paré-Blagoev, Insler, & Wagner, 2005; Badre & Wagner, 2007; Dobbins et al., 2002; Hasegawa, Hayashi, & Miyashita, 1999; Wagner, Paré-Blagoev, Clark, & Poldrack, 2001).

The second goal of our study was to determine whether bottom-up and top-down information flow between the MTL and the PFC and posterior parietal cortex (PPC) are similarly impacted by MTL stimulation. Multiple lines of evidence across species have revealed a role for the PPC in episodic memory (Cabeza, 2008; Cabeza, Ciaramelli, & Moscovitch, 2012; Cabeza et al., 2008; Cabeza et al., 2011; Hutchinson, Uncapher, & Wagner, 2009; Uncapher & Wagner, 2009; Wagner et al., 2005). Anterograde and retrograde tracing studies in non-human primates have uncovered projections from the MTL to the PPC (Clower, West, Lynch, & Strick, 2001; Insausti & Muñoz, 2001) and in the reverse direction (Rockland & Van Hoesen, 1999). Single-neuron studies in rodents (Chen, Lin, Green, Barnes, & McNaughton, 1994; McNaughton et al., 1994; Nitz, 2006) as well as non-human primates (Andersen, Essick, & Siegel, 1985; Crowe, Chafee, Averbeck, & Georgopoulos, 2004) have established PPC involvement in spatial memory. fMRI studies in non-human primates have reported coactivation of the MTL and PPC during successful memory encoding and recall (Miyamoto et al., 2013).

Studies using resting-state fMRI in humans have confirmed intrinsic MTL connectivity with the PPC (Vincent et al., 2006). Other human fMRI studies have reported dorsal PPC activation during episodic memory retrieval (Buckner et al., 1998; Konishi, Wheeler, Donaldson, & Buckner, 2000), spatial memory processing (Amorapanth, Widick, & Chatterjee, 2010; Baumann, Chan, & Mattingley, 2012), and coactivation of the hippocampus and multiple subdivisions of the PPC during episodic and semantic memory encoding and retrieval (Ciaramelli, Burianová, Vallesi, Cabeza, & Moscovitch, 2020; Gurd et al., 2002; Vincent et al., 2006). The dorsal PPC is involved in top-down attention processing during memory encoding (Cabeza, 2008; Cabeza et al., 2012; Cabeza et al., 2011; Ciaramelli, Grady, & Moscovitch, 2008;

Daselaar et al., 2009; Hutchinson et al., 2009; Uncapher & Wagner, 2009). Human electrocorticography studies have suggested a role for the PPC in verbal episodic memory encoding and recall (Gonzalez et al., 2015) and human iEEG studies have found that hippocampus-PPC correlation in the theta frequency band is prominent in spatial memory (Ekstrom et al., 2005). Together, these findings suggest that coordinated interactions between the MTL and PPC play a role in episodic memory. However, the causal role of MTL-PPC circuits remains poorly understood and it is not known whether MTL stimulation alters directed information flow between MTL and PPC differently from the PFC.

Our analyses reveal how MTL stimulation alters frequency-specific bottom-up and top-down information flow between the MTL and PFC and how this differs from PPC regions implicated in human episodic memory. Findings provide new insights into causal mechanisms involved in the operation of human episodic memory circuits.

Materials and Methods

UPENN-RAM iEEG recordings

iEEG recordings from 14 patients (10 females, 4 males) shared by Kahana and colleagues at the University of Pennsylvania (UPENN) (obtained from the UPENN-RAM public data release) were used for analysis (Goyal et al., 2018; Jacobs et al., 2016). Patients with pharmaco-resistant epilepsy underwent surgery for removal of their seizure onset zones. iEEG recordings of these patients were downloaded from a UPENN-RAM consortium hosted data sharing archive (URL: http://memory.psych.upenn.edu/RAM). Prior to data collection, research protocols and ethical guidelines were approved by the Institutional Review Board at the participating hospitals and

283 informed consent was obtained from the participants and guardians (Jacobs et al., 2016). Details
284 of all the recordings sessions and data pre-processing procedures are described by Kahana and
285 colleagues (Jacobs et al., 2016). Briefly, iEEG recordings were obtained using subdural grids and
286 strips (contacts placed 10 mm apart) or depth electrodes (contacts spaced 5–10 mm apart) using
287 recording systems at each clinical site. iEEG systems included DeltaMed XlTek (Natus), Grass
288 Telefactor, and Nihon-Kohden EEG systems. These patients performed a verbal episodic
289 memory task (see below) and received direct brain stimulation during some of the encoding
290 trials. Electrodes located in brain lesions or those which corresponded to seizure onset zones or
291 had significant interictal spiking or had broken leads, were excluded from analysis.
292
293 Anatomical localization of electrode placement was accomplished by co-registering the
294 postoperative computed CTs with the postoperative MRIs using FSL (FMRIB (Functional MRI
295 of the Brain) Software Library), BET (Brain Extraction Tool), and FLIRT (FMRIB Linear Image
296 Registration Tool) software packages. Preoperative MRIs were used when postoperative MRIs
297 were not available. The resulting contact locations were mapped to MNI space using an indirect
298 stereotactic technique and OsiriX Imaging Software DICOM viewer package. We used the
299 Brainnetome atlas (Fan et al., 2016) to demarcate bihemispheric middle and inferior frontal
300 gyrus subdivisions of the prefrontal cortex (MFG and IFG) and dorsal and ventral subdivisions
301 of the posterior parietal cortex (dPPC and vPPC) as well as the hippocampus, parahippocampal
302 gyrus, and entorhinal cortex subdivisions of the MTL. We first identified electrode pairs in
303 patients with electrodes implanted in each pair of brain regions of interest (for example, MTL-
304 MFG). Key PPC regions of interest included the superior parietal lobule, and supramarginal
305 gyrus, intraparietal sulcus and angular gyrus in the inferior parietal lobule, spanning its dorsal-

ventral axis. The lack of sufficient number of participants and electrode pairs precluded analyses of these subdivisions separately. We therefore combined electrodes from the superior parietal lobule, intraparietal sulcus, and supramarginal gyrus into a dorsal PPC subdivision and the angular gyrus regions into a ventral PPC subdivision (**Tables 2, 3**). Ages of these patients ranged from 20 to 49, with mean age 36.0 ± 10.1 and the dataset included 10 females. Gender differences were not analyzed in this study due to lack of sufficient male participants for electrodes pairs for MTL-MFG, MTL-IFG, MTL-dPPC, and MTL-vPPC interactions (**Table 2**).

Original sampling rates of iEEG signals were 500 Hz, 1000 Hz, and 1600 Hz. Hence, iEEG signals were downsampled to 500 Hz, if the original sampling rate was higher, for all subsequent analysis. The two major concerns when analyzing interactions between closely spaced intracranial electrodes are volume conduction and confounding interactions with the reference electrode (Burke et al., 2013). Hence bipolar referencing was used to eliminate confounding artifacts and improve the signal-to-noise ratio of the neural signals, consistent with previous studies using UPENN-RAM iEEG data (Burke et al., 2013; Ezzyat et al., 2018). Signals recorded at individual electrodes were converted to a bipolar montage by computing the difference in signal between adjacent electrode pairs on each strip, grid, and depth electrode and the resulting bipolar signals were treated as new "virtual" electrodes originating from the midpoint between each contact pair, identical to procedures in previous studies using UPENN-RAM data (Solomon et al., 2019). Line noise (60 Hz) and its harmonics were removed from the bipolar signals and finally each bipolar signal was Z-normalized by removing mean and scaling by the standard deviation. For filtering, we used a fourth order two-way zero phase lag Butterworth filter throughout the analysis.

329

330 ***iEEG verbal free recall task and stimulation paradigm***

331

332 Patients performed multiple trials of a free recall experiment, where they were presented with a
333 list of words and subsequently asked to recall as many as possible from the original list (**Figure**
334 **1c**) (Solomon et al., 2017; Solomon et al., 2019). Each session consisted of 25 lists. The task
335 consisted of three periods: encoding, delay, and recall. During encoding, a list of 12 words was
336 visually presented for ~30 sec. Words were selected at random, without replacement, from a pool
337 of high frequency English nouns (http://memory.psych.upenn.edu/Word_Pools). Each word was
338 presented for a duration of 1600 msec, followed by an inter-stimulus interval of 800 to 1200
339 msec. After a 20 sec post-encoding delay where participants performed a series of distractor
340 tasks consisting of arithmetic problems of the form $a+b+c=?$, where a, b, and, c were randomly
341 chosen integers from 1 to 9, participants were instructed to recall as many words as possible
342 during the 30 sec recall period.

343

344 For each subject, a selected electrode pair in the MTL was connected to an electrical stimulator
345 (Grass Technologies or Blackrock Microsystems) and stimulation was applied using parameters
346 from a prior study (Suthana et al., 2012), showing a positive effect of stimulation on memory
347 performance. Subjects were instructed about the stimulation procedure but were blinded to the
348 location of the stimulation sites. Bipolar-symmetric, charge-balanced, square-wave stimulation
349 current between a pair of electrodes was applied at 50 Hz and 300 μs pulse-width. All the
350 stimulation electrodes in the present study were depth electrodes. Safe amplitude for stimulation
351 was determined at the start of each session under a clinically supervised mapping procedure by

manually testing a range of currents for each site, beginning at 0.25 mA and slowly increasing to a maximum of 1.5 mA. The final stimulation current (**Table 1**) that was used for the cognitive experiments was the maximum current for each site that could be applied without inducing patient symptoms, epileptiform after discharges, or seizures. We designated a stimulation site being in the MTL if at least one electrode of the bipolar pair was in the region.

For the stimulated lists, exactly half of the words on the list were delivered simultaneously with electrical brain stimulation. For the control lists, all 12 words on the list were presented without stimulation. Out of the 25 lists in each session, 20 were stimulated lists and 5 were control lists in a randomly assigned order. For each stimulated list, stimulation occurred in a blocked pattern: the stimulator was active during the presentation of a pair of consecutive words and then inactive for the following pair. Thus, in total, on each stimulated list, the stimulator was active for half the total words. For the stimulation blocks, the stimulator was timed to occur 200 msec before the presentation of the first word in each block, continuing for 4.6 s, until the disappearance of the second word. The onset of stimulation was balanced, such that a random half of the stimulation lists began with a non-stimulated block and the others began with a stimulated block.

We analyzed 1600 msec iEEG epochs from the encoding periods of the free recall task. For the recall periods, iEEG recordings 1600 msec prior to the vocal onset of each word were analyzed (Solomon et al., 2019). Data from each trial was analyzed separately and specific measures were averaged across trials. Effects of electrical stimulation on behavioral performance has been analyzed in detail by Kahana and colleagues elsewhere (Goyal et al., 2018; Jacobs et al., 2016). Our major focus in this study was on the effect of stimulation on the direction of information

flow between the MTL and the PFC and PPC. The mismatch in the number of trials between successfully versus unsuccessfully encoded words (roughly 1:3) made it difficult to directly compare causal signaling measures associated with the two. From the point of view of probing behaviorally effective memory encoding, our focus was therefore on how MTL stimulation affects successful encoding and recall, consistent with most prior studies (Long, Burke, & Kahana, 2014; Watrous et al., 2013). For stimulation trials, data corresponding to the pair of words immediately succeeding the stimulated word pair was analyzed. Data corresponding to the stimulated word pair were excluded from analysis to prevent contamination with stimulation artifact (Hansen et al., 2018; Jun, Lee, Kim, Jeong, & Chung, 2020; Kucewicz, Berry, Miller, et al., 2018).

Control analysis using resting-state iEEG data with MTL stimulation

For the control condition, we used "resting-state" data from 2 participants collected in the UPENN-RAM public data release (Solomon et al., 2021). These patients were part of a larger "parameter search" project whose major goal was to systematically study the effects of stimulation frequency, current, and stimulation brain regions (Mohan et al., 2020). We reanalyzed iEEG data from these participants to determine whether the main findings of directed information flow between the MTL and the PFC and PPC in our study were due to brain stimulation causing reorganization of brain circuits and thus influencing the information flow that we observed in the memory task. Similar to the memory task, bipolar-symmetric, charge-balanced, square-wave stimulation current between a pair of depth MTL electrodes was applied at 50 Hz and 300 μs pulse-width (also see **Table 6**). Similar procedures were adopted for

398 determining the safe current amplitude for stimulation for these participants. Based on electrode
399 placement in the MTL and the PFC and PPC brain regions and based on the criteria that the
400 stimulation frequency was 50 Hz, we selected 2 subjects with simultaneous electrode placements
401 in MTL and MFG (100 electrode pairs) and also MTL and dPPC (60 electrode pairs). IFG and
402 vPPC were excluded from analysis due to lack of electrode placements in these regions. The
403 stimulation duration for these two subjects were 250 msec and 500 msec (**Table 6**).
404
405 We analyzed 1600 msec iEEG epochs immediately prior to the start of each stimulation trial;
406 these correspond to the "non-stim" condition. We also analyzed 1600 msec iEEG epochs
407 immediately after the end of each stimulation trial; these correspond to the "stim" condition.
408 Trials were spaced by 3 s, with up to ± 200 msec of randomly-applied jitter added to the interval.
409 Subjects were instructed to sit quietly and did not perform any task. Similar to the memory task,
410 data from each trial was analyzed separately and PTE measures were averaged across trials. Data
411 corresponding to the stimulated epochs were excluded from analysis to prevent contamination
412 with stimulation artifact (Hansen et al., 2018; Jun et al., 2020; Kucewicz, Berry, Miller, et al.,
413 2018).
414
415 ***iEEG analysis of power***
416
417 For power analysis, we first filtered the signals in the delta-theta (0.5-8 Hz) and beta (12-30 Hz)
418 frequency bands and then calculated the square of the filtered signals as the power of the signals
419 (Kwon et al., 2021). Signals were then smoothed using 0.2 sec windows with 90% overlap
420 (Kwon et al., 2021) and normalized with respect to 0.2 sec pre-stimulus periods.

iEEG analysis of phase transfer entropy (PTE) and direction of information flow

Phase transfer entropy (PTE) is a nonlinear measure of the directionality of information flow between time-series and can be applied to nonstationary time-series (Das & Menon, 2020; Lobier et al., 2014). Note that information flow described here relates to signaling between brain areas and does not necessarily reflect the repsresentation or coding of behaviorally relevant variables per se. The PTE measure is in contrast to the Granger causality measure which can be applied only to stationary time-series (Barnett & Seth, 2014). We first carried out a stationarity test of the iEEG recordings (unit root test for stationarity (Barnett & Seth, 2014)) and found that the spectral radius of the autoregressive model is very close to one, indicating that the iEEG time-series is nonstationary. This precluded the applicability of the Granger causality analysis in our study.

Given two time-series $\{x_i\}$ and $\{y_i\}$, where $i = 1,2,...,M$, instantaneous phases were first extracted using the Hilbert transform. Let $\{x_i^p\}$ and $\{y_i^p\}$, where $i = 1,2,...,M$, denote the corresponding phase time-series. If the uncertainty of the target signal $\{y_i^p\}$ at delay τ is quantified using Shannon entropy, then the PTE from driver signal $\{x_i^p\}$ to target signal $\{y_i^p\}$ can be given by

$$PTE_{x\to y} = \sum_i p\left(y_{i+\tau}^p, y_i^p, x_i^p\right) \log\left(\frac{p\left(y_{i+\tau}^p \mid y_i^p, x_i^p\right)}{p\left(y_{i+\tau}^p \mid y_i^p\right)}\right), \quad \text{(i)}$$

where the probabilities can be calculated by building histograms of occurrences of singles, pairs, or triplets of instantaneous phase estimates from the phase time-series (Hillebrand et al., 2016).

For our analysis, the number of bins in the histograms was set as $3.49\times STD\times M^{-1/3}$ and delay τ was set as $2M/M_{\pm}$, where STD is average standard deviation of the phase time-series $\{x_i^p\}$ and $\{y_i^p\}$ and $M_{\pm}$ is the number of times the phase changes sign across time and channels (Hillebrand et al., 2016). PTE has been shown to be robust against the choice of the delay τ and the number of bins for forming the histograms (Hillebrand et al., 2016).

iEEG analysis of phase locking value (PLV) and phase synchronization

We used phase locking value (PLV) to compute phase synchronization between two time-series (Lachaux, Rodriguez, Martinerie, & Varela, 1999). We first calculated the instantaneous phases of the two signals by using the analytical signal approach based on the Hilbert transform (Bruns, 2004). Given time-series $x(t),\ t=1,2,...,M$, its complex-valued analytical signal $z(t)$ can be computed as

$$z(t)=x(t)+i\tilde{x}(t)=A_x(t)e^{\Phi_x(t)}, \qquad \text{(i)}$$

where i denotes the square root of minus one, $\tilde{x}(t)$ is the Hilbert transform of $x(t)$, and $A_x(t)$ and $\Phi_x(t)$ are the instantaneous amplitude and instantaneous phase respectively and can be given by

$$A_x(t)=\sqrt{[x(t)]^2+[\tilde{x}(t)]^2} \quad \text{and} \quad \Phi_x(t)=\arctan\frac{\tilde{x}(t)}{x(t)}. \qquad \text{(ii)}$$

The Hilbert transform of $x(t)$ was computed as

$$\tilde{x}(t) = \frac{1}{\pi} PV \int_{-\infty}^{\infty} \frac{x(\tau)}{t-\tau} d\tau \ , \qquad \text{(iii)}$$

where PV denotes the Cauchy principal value. MATLAB function "hilbert" was used to calculate the Hilbert transform in our analysis. Given two time-series $x(t)$ and $y(t)$, where $t = 1, 2, ..., M$, the PLV (zero-lag) can be computed as

$$PLV = \left| E\left[e^{i(\Phi_x(t) - \Phi_y(t))} \right] \right| \ , \qquad \text{(iv)}$$

where $\Phi_y(t)$ is the instantaneous phase for time-series $y(t)$, $|\cdot|$ denotes the absolute value operator, $E[\cdot]$ denotes the expectation operator with respect to time t, and i denotes the square root of minus one. PLVs were then averaged across trials to estimate the final PLV for each pair of electrodes.

iEEG analysis of modulation index and phase-amplitude coupling (PAC)

We used the modulation index estimation procedure (Tort et al., 2008) to calculate phase-amplitude coupling (PAC) of electrodes. We first denote the amplitude and the phase frequency ranges for our analysis by f_A ([80, 160] Hz) and fp ([0.5, 8] Hz), respectively. Let $x(t)$ denote the time-series of the electrode. We first filter $x(t)$ at the two frequency ranges f_A and fp. Let's denote the filtered signals as $x_{fA}(t)$ and $x_{fp}(t)$ respectively. We then estimate the phase time-series $\varphi_{fp}(t)$ from the Hilbert transform of $x_{fp}(t)$ and the amplitude time-series $A_{fA}(t)$ from the Hilbert

transform of $x_{fA}(t)$. Each point in the composite time-series $[\varphi_{fp}(t), A_{fA}(t)]$ indicates an amplitude of an oscillation in f_A at the corresponding phase in the fp oscillation. We next bin the phases $\varphi_{fp}(t)$ into eighteen 20^0 intervals (0^0 to 360^0) and calculate the mean of A_{fA} over each of the phase bins. Let's $\langle A_{fA}\rangle_{\varphi_{fp}}(j)$ denote the mean A_{fA} value at each phase bin j. We then define entropy H as

$$H = -\sum_{j=1}^{N} p_j \log p_j ,$$

where $N = 18$ is the number of phase bins and p_j is given by

$$p_j = \frac{\langle A_{fA}\rangle_{\varphi_{fp}}(j)}{\sum_{j=1}^{N}\langle A_{fA}\rangle_{\varphi_{fp}}(j)}.$$

The MI is estimated by normalizing H by the maximum possible entropy value H_{max} which is obtained for the uniform distribution $p_j = 1/N$ ($H_{max} = \log N$):

$$MI = \frac{H_{max} - H}{H_{max}}.$$

Higher MI values indicate stronger PAC with zero MI corresponding to zero PAC.

Statistical analysis

Statistical analysis was conducted using mixed effects analysis with the *lmerTest* package (Kuznetsova, Brockhoff, & Christensen, 2017) implemented in R software (version 4.0.2, R Foundation for Statistical Computing). Because PTE data were not normally distributed, we used BestNormalize (Peterson & Cavanaugh, 2018) which contains a suite of transformation-estimating functions that can be used to optimally normalize data. The resulting normally distributed data were subjected to mixed effects analysis with the following model: *PTE ~ Condition + (1|Subject)*, where *Condition* models the fixed effects (condition differences) and (1|*Subject*) models the random repeated measurements within the same participant. Analysis of variance (ANOVA) was used to test the significance of findings with FDR-corrections for multiple comparisons ($p<0.05$). Analysis of power, PLV, and PAC were carried out in the same manner using the mixed effects analysis.

The differential effects of stimulation on directed information flow between the MTL and the MFG, IFG, dPPC, and vPPC was also tested with a 2-way ANOVA with the factors Region (MFG, IFG, dPPC, and vPPC) and Stimulation (ON/OFF). Linear mixed effects analysis was run in a similar way, with the following model: *PTE ~ Stimulation* x *Region + (1|Subject)*. 2-way ANOVA was then used to test the significance of findings with FDR-corrections for multiple comparisons ($p<0.05$).

For effect size estimation, we used η^2 statistics for complex F-based effects such as interactions effects and main effects with multiple factors and Cohen's *d* statistics for pairwise post-hoc

comparisons. We used the *eta_squared()* function in the *effectsize* package implemented in R for estimating η^2 and the *lme.dscore()* function in the *EMAtools* package in R for estimating Cohen's *d*.

We also conducted surrogate analysis to test the significance of the estimated PTE values (Hillebrand et al., 2016). The estimated phases from the Hilbert transform for electrodes from a given pair of brain areas were time-shuffled so that the predictability of one time-series from another is destroyed, and PTE analysis was repeated on this shuffled data to build a distribution of surrogate PTE values against which the observed PTE was tested ($p<0.05$).

Results

Behavioral effects of MTL stimulation

Participants were presented with a sequence of words and asked to remember them for subsequent recall (**Methods**, **Tables 1-3**, **Figure 1**) (Solomon et al., 2019). During encoding, a list of 12 words was visually presented for ~30 s. Each word was presented for a duration of 1600 msec, followed by an inter-stimulus interval of 800 to 1200 msec. After a ~20 sec post-encoding delay, participants were instructed to recall as many words as possible from the original list during the 30 sec recall period. MTL stimulation occurred in a blocked pattern: the stimulator was active during the presentation of a pair of consecutive words and then inactive for the following pair.

Average memory recall accuracy across patients was 22.9% ± 11.7% for MTL stimulation trials and 27.5% ± 12.9% for non-stimulation trials. Memory recall was lower on stimulation,

compared to non-stimulation, trials, this difference was marginally significant (p = 0.0574, Cohen's d = 0.51, Wilcoxon signed-rank test). This result is consistent with prior studies using UPENN-RAM data (Goyal et al., 2018; Jacobs et al., 2016; Kucewicz, Berry, Kremen, et al., 2018) as well as other reports that direct stimulation of the hippocampus generally impairs memory (Chua & Ahmed, 2016; Coleshill et al., 2004; Fernandez, Hufnagel, Helmstaedter, Zentner, & Elger, 1996; Halgren, Wilson, & Stapleton, 1985; Herweg, Solomon, & Kahana, 2020; Jackson, Feredoes, Rich, Lindner, & Woolgar, 2021; Jun et al., 2020; Lacruz et al., 2010; Merkow et al., 2017).

Effect of MTL stimulation on information flow from MTL to PFC and PPC during memory encoding

We examined the differential effects of stimulation on directed information flow from the MTL to MFG, IFG, dorsal PPC (dPPC), and ventral PPC (vPPC), using a 2-way ANOVA with the factors Region (MFG, IFG, dPPC, and vPPC) and Stimulation (ON/OFF) (**Methods**). We focused on directed information flow from the MTL to the PFC and PPC, in the delta-theta and beta bands, based on our replicable findings across verbal and spatial memory domains (Das & Menon, 2021, 2022). To preclude confounding influences associated with unsuccessful recall, we focused on how MTL stimulation affects encoding and recall on successful trials, consistent with prior studies (Long et al., 2014; Watrous et al., 2013). We found no interaction between Stimulation and Region in either delta-theta ($F(1, 660) = 0.06$, $p>0.05$, η^2 = 9.76e-05) or beta ($F(1, 663) = 0.68$, $p>0.05$, η^2 = 1.02e-03) frequency bands during memory encoding. We also did not find any main effects of Stimulation in either delta-theta ($F(1, 660) = 3.99$, $p>0.05$, η^2 =

579 6.01e-03) or beta ($F(1, 663) = 0.06$, $p>0.05$, $\eta^2 = 9.76e-05$) frequency bands during memory
580 encoding (**Table 4**).
581
582 *Effect of MTL stimulation on information flow to the MTL from the PFC and PPC during*
583 *memory encoding*
584
585 We next examined directed information flow to the MTL from the PFC and PPC during verbal
586 memory encoding. We examined the differential effects of stimulation on directed information
587 flow from the MFG, IFG, dPPC, and vPPC to the MTL, using a 2-way ANOVA with factors
588 Region (MFG, IFG, dPPC, and vPPC) and Stimulation (ON/OFF) (**Methods**). We found a
589 significant Stimulation x Region interaction for directed information flow from the PFC and PPC
590 to the MTL in the delta-theta band, ($F(1, 663) = 11.75$, $p<0.01$, $\eta^2 = 0.02$) (**Table 4**). There was
591 no interaction between Stimulation and Region ($F(1, 663) = 0.67$, $p>0.05$, $\eta^2 = 1.01e-03$), or
592 main effect of Stimulation ($F(1, 663) = 1.04$, $p>0.05$, $\eta^2 = 1.57e-03$) in the beta frequency band
593 (**Table 4**).
594
595 Next, we conducted post-hoc tests to systematically investigate regional differences in the effects
596 of MTL stimulation on directed information flow to the MTL in the delta-theta band (**Figure 2**).
597 MFG→MTL directed information flow decreased during stimulation trials compared to non-
598 stimulation trials in the delta-theta band ($F(1, 260) = 12.00$, $p<0.01$, Cohen's $d = 0.43$) (**Figure**
599 **2**). In contrast, IFG→MTL ($F(1, 130) = 0.42$, $p>0.05$, Cohen's $d = 0.11$), dorsal PPC→MTL
600 ($F(1, 220) = 0.45$, $p>0.05$, Cohen's $d = 0.09$), and ventral PPC→MTL ($F(1, 42) = 3.36$, $p>0.05$,
601 Cohen's $d = 0.57$) directed information flow did not differ between stimulation and non-

stimulation trials. We then compared the strength of top-down information flow to the MTL from the MFG, and dorsal and ventral PPC, associated with MTL stimulation. MFG→MTL directed information flow did not differ from dorsal PPC→MTL ($F(1, 28) = 0.03$, $p>0.05$, Cohen's $d = 0.07$) and ventral PPC→MTL ($F(1, 137) = 0.17$, $p>0.05$, Cohen's $d = 0.07$) directed information flow on stimulation trials.

These results demonstrate that MTL stimulation reduces top-down MFG→MTL information flow in the delta-theta band during memory encoding, and that this effect is specific to PFC with no differences in either the dorsal or ventral PPC.

Effect of MTL stimulation on information flow from MTL to PFC and PPC during memory recall

We next examined the differential effects of stimulation on directed information flow from the MTL to the MFG, IFG, dPPC, and vPPC, with a 2-way ANOVA with the factors Region (MFG, IFG, dPPC, and vPPC) and Stimulation (ON/OFF) during the memory recall period which occurred ~20 sec after word encoding (**Methods**). There was no significant Stimulation x Region interaction in the delta-theta band ($F(1, 662) = 2.64$, $p>0.05$, $\eta^2 = 3.98e-03$) (**Table 4**). However, there was a main effect of Stimulation, with higher directed information flow from the MTL to the PFC and PPC during trials with stimulation ($F(1, 662) = 7.19$, $p<0.05$, $\eta^2 = 0.01$). There was no Stimulation x Region interaction ($F(1, 663) = 5.61$, $p=0.05$, $\eta^2 = 8.39e-03$) or main effect of Stimulation ($F(1, 663) = 4.62$, $p>0.05$, $\eta^2 = 6.91e-03$) in the beta-band (**Table 4**).

Effect of MTL stimulation on information flow to MTL from PFC and PPC during memory recall

We next examined the differential effects of stimulation on directed information flow from the MFG, IFG, dPPC, and vPPC to the MTL, with a 2-way ANOVA with the factors Region (MFG, IFG, dPPC, and vPPC) and Stimulation (ON/OFF) during the memory recall period (**Methods**). In the delta-theta band, we found no significant Stimulation x Region interaction ($F(1, 663) = 0.00$, $p>0.05$, $\eta^2 = 1.49e\text{-}06$) or main effect of Stimulation ($F(1, 663) = 0.78$, $p>0.05$, $\eta^2 = 1.18e\text{-}03$) (**Table 4**).

We found a significant Stimulation x Region interaction for directed information flow from PFC and PPC to MTL in the beta-band ($F(1, 663) = 11.92$, $p<0.01$, $\eta^2 = 0.02$) (**Table 4**). Post-hoc analysis of this interaction revealed that MFG→MTL directed information flow decreased during stimulation, compared to the non-stimulation, trials ($F(1, 260) = 11.11$, $p<0.01$, Cohen's $d = 0.41$) (**Figure 3**). In contrast, IFG→MTL ($F(1, 130) = 3.75$, $p>0.05$, Cohen's $d = 0.34$), dorsal PPC→MTL ($F(1, 220) = 1.93$, $p>0.05$, Cohen's $d = 0.19$), and ventral PPC→MTL ($F(1, 41) = 0.48$, $p>0.05$, Cohen's $d = 0.22$) information flow did not differ between stimulation and non-stimulation trials. We then compared the strength of top-down information flow to the MTL from the MFG and dorsal PPC associated with MTL stimulation. This analysis revealed that MFG→MTL directed information flow was significantly lower than dorsal PPC→MTL information flow on stimulation trials ($F(1, 213) = 10.02$, $p<0.01$, Cohen's $d = 0.43$) (**Figure 4**). MFG→MTL directed information flow did not differ from dorsal PPC→MTL information flow during non-stimulation trials ($F(1, 104) = 3.50$, $p>0.05$, Cohen's $d = 0.37$). MFG→MTL directed information flow was lower than ventral PPC→MTL information flow during both stimulation

($F(1, 149) = 17.23$, $p<0.001$, Cohen's $d = 0.68$) (**Figure 4**) and non-stimulation trials ($F(1, 142) = 10.26$, $p<0.01$, Cohen's $d = 0.56$).

Together, these results suggest that MTL stimulation reduces top-down directed information flow from the MFG subdivision of the PFC to the MTL in the beta band during memory recall. Results further suggest that MTL stimulation selectively suppresses top-down influences from the MFG, compared to both dorsal and ventral PPC, and that the PFC is relatively more sensitive to the effects of stimulation compared to the PPC.

Effect of MTL stimulation on information flow between the MTL and the PFC and PPC in resting state

To determine whether our main findings related to the direction of information flow between the MTL and the PFC and PPC in our study were specific to the effects of memory processing, we used "resting-state" data from participants collected in the UPENN-RAM public data release (Solomon et al., 2021). Subjects were instructed to sit quietly and did not perform any task. Similar to the memory task, bipolar stimulation current between pairs of depth MTL electrodes was applied at 50 Hz (**Table 6**). Based on electrode placement in the MTL and the PFC and PPC brain regions and based on the criteria that the stimulation frequency was 50 Hz, we selected 2 subjects (n=105 electrode pairs for MFG and n=60 electrode pairs for dPPC; IFG and vPPC did not have electrode sampling) with simultaneous electrode placements in MTL and MFG and also MTL and dPPC. We analyzed 1600 msec iEEG epochs immediately prior to the start of each stimulation trial; these correspond to the "non-stim" condition. We also analyzed 1600 msec

iEEG epochs immediately after the end of each stimulation trial; these correspond to the "stim" condition.

We found that, in contrast to the memory task, neither MTL→MFG ($F(1, 207) = 0.04$, $p>0.05$, Cohen's $d = 0.03$) nor MFG→MTL ($F(1, 207) = 0.00$, $p>0.05$, Cohen's $d = 0.00$) directed information flow changed during stimulation, compared to the non-stimulation, trials in the delta-theta frequency band. Moreover, neither MTL→MFG ($F(1, 207) = 1.44$, $p>0.05$, Cohen's $d = 0.17$) nor MFG→MTL ($F(1, 207) = 3.35$, $p>0.05$, Cohen's $d = 0.25$) directed information flow changed during stimulation, compared to the non-stimulation, trials in the beta frequency band.

Furthermore, we found that, neither MTL→dPPC nor dPPC→MTL directed information flow changed during stimulation, compared to the non-stimulation, trials in both the delta-theta ($F(1, 117) = 1.69$, $p>0.05$, Cohen's $d = 0.24$ for MTL→dPPC and $F(1, 117) = 0.08$, $p>0.05$, Cohen's $d = 0.05$ for dPPC→MTL) and beta ($F(1, 117) = 0.01$, $p>0.05$, Cohen's $d = 0.02$ for MTL→dPPC and $F(1, 117) = 0.84$, $p>0.05$, Cohen's $d = 0.17$ for dPPC→MTL) frequency bands.

Together, these results suggest that the reported results related to direction of information flow between the MTL and the PFC and PPC that we observed during the memory task, cannot be solely attributable to effects of brain stimulation causing reorganization of brain circuits, rather they are related to the combined effects of stimulation and memory processing.

Comparison of information flow between the MTL and the PFC and PPC during memory processing and resting state

694 To provide further evidence that our main findings related to the direction of information flow
695 between the MTL and the PFC and PPC were specific to the effects of memory processing, we
696 directly compared information flow from the MTL to the PFC and PPC, and the reverse, for the
697 memory encoding and recall conditions with the resting-state condition, during the stimulation
698 trials.
699
700 We first focused our analysis on bottom-up directed information flow from the MTL to the PFC
701 and PPC. This analysis revealed that MTL→MFG directed information flow was higher for both
702 memory encoding ($F(1, 235) = 8.34$, $p<0.01$, Cohen's $d = 0.38$) and recall ($F(1, 115) = 23.72$,
703 $p<0.001$, Cohen's $d = 0.91$) compared to rest, during stimulation in the delta-theta frequency
704 band. This finding was reversed in the beta frequency band, where MTL→MFG directed
705 information flow was lower for both memory encoding ($F(1, 233) = 16.33$, $p<0.001$, Cohen's $d =$
706 0.53) and recall ($F(1, 233) = 36.70$, $p<0.001$, Cohen's $d = 0.79$) compared to rest. MTL→dPPC
707 directed information flow was higher for both memory encoding ($F(1, 170) = 29.73$, $p<0.001$,
708 Cohen's $d = 0.83$) and recall ($F(1, 161) = 39.08$, $p<0.001$, Cohen's $d = 0.99$) compared to rest,
709 during stimulation in the delta-theta frequency band. MTL→dPPC directed information flow was
710 also higher for memory recall ($F(1, 169) = 5.75$, $p<0.05$, Cohen's $d = 0.37$) compared to rest,
711 during stimulation in the beta band, however, MTL→dPPC directed information flow did not
712 differ for memory encoding and rest conditions in the beta band ($F(1, 170) = 0.08$, $p>0.05$,
713 Cohen's $d = 0.04$). These results suggest that the "bottom-up" effects of stimulation on memory
714 processing enhance MTL to PFC information flow in the delta-theta frequency band and
715 suppress this information flow in the beta frequency band, compared to rest. On the other hand,

716 the “bottom-up” effects of stimulation on memory processing enhance MTL to PPC information
717 flow in both delta-theta and beta frequency bands, compared to rest.
718
719 We next examined top-down directed information flow from the PFC and PPC to the MTL. This
720 analysis revealed that MFG→MTL directed information flow was lower for both memory
721 encoding ($F(1, 172) = 42.28$, $p<0.001$, Cohen's $d = 0.99$) and recall ($F(1, 181) = 35.23$, $p<0.001$,
722 Cohen's $d = 0.88$) compared to rest, in the delta-theta frequency band and for memory recall
723 compared to rest, in the beta frequency band ($F(1, 235) = 47.55$, $p<0.001$, Cohen's $d = 0.90$).
724 MFG→MTL directed information flow did not differ between memory encoding and rest in the
725 beta band ($F(1, 235) = 0.05$, $p>0.05$, Cohen's $d = 0.03$). dPPC→MTL directed information flow
726 was lower for both memory encoding ($F(1, 21) = 15.00$, $p<0.01$, Cohen's $d = 1.67$) and recall
727 ($F(1, 172) = 14.26$, $p<0.001$, Cohen's $d = 0.58$) compared to rest, in the delta-theta frequency
728 band. dPPC→MTL directed information flow was higher for memory encoding ($F(1, 161) =$
729 15.46, $p<0.001$, Cohen's $d = 0.62$), but lower for memory recall ($F(1, 172) = 13.41$, $p<0.001$,
730 Cohen's $d = 0.56$) compared to rest, during stimulation in the beta band. These results suggest
731 that the “top-down” effects of stimulation on memory processing mostly suppress information
732 flow from the PFC and PPC to the MTL compared to rest.
733
734 Together, these results provide further evidence that the reported results related to direction of
735 information flow between the MTL and the PFC and PPC, during the memory task, cannot be
736 solely attributable to effects of brain stimulation causing reorganization of brain circuits. Rather,
737 they are related to the combined effects of stimulation and memory processing.
738

Effect of MTL stimulation on directed information flow for successful vs. unsuccessful memory recall

We next examine the effect of stimulation on directed information flow for successful compared to unsuccessful memory trials. To directly examine behavioral effects of stimulation, we focus our results on the memory recall periods (**Table 5**) (but see **Table 5** for results related to the memory encoding periods where strong behavioral signatures were absent). This analysis revealed that MTL→MFG directed information flow was significantly lower for successful, compared to unsuccessful, memory recall in the beta band ($F(1, 259) = 18.50$, $p<0.001$, Cohen's $d = 0.53$) (**Figure 5**). MTL→vPPC directed information flow was significantly higher for successful, compared to unsuccessful, memory recall in both delta-theta ($F(1, 41) = 24.01$, $p<0.001$, Cohen's $d = 1.62$) and beta ($F(1, 41) = 10.27$, $p<0.01$, Cohen's $d = 0.77$) frequency bands (**Figure 5**).

Together, these results suggest that the strongest behavioral effects of MTL stimulation are in the bottom-up direction, mediating information flow from MTL to MFG and vPPC. Results also suggest that both stimulation and memory processing contribute to directed information flow between the MTL and the PFC and PPC that we observed during the memory task.

Surrogate data analysis of directed information flow between the MTL and the PFC and PPC

Next, we conducted surrogate data analysis to test the significance of the estimated PTE values compared to PTE expected by chance (**Methods**) for the stimulation trials. The estimated phases

762 from the Hilbert transform for electrodes from pairs of brain areas were time-shuffled and PTE
763 analysis was repeated on this shuffled data to build a distribution of surrogate PTE values against
764 which the observed PTE was tested.
765
766 Surrogate data analysis revealed that directed information flow from the MTL to MFG, IFG,
767 dorsal PPC, and ventral PPC and in the reverse direction, were significantly higher than those
768 expected by chance ($p<0.05$ in all cases) in the delta-theta frequency band during both memory
769 encoding and recall periods. In contrast, in the beta frequency band, directed information flow
770 from the MTL to PFC and PPC subdivisions, and in the reverse direction, were significantly
771 lower than those expected by chance ($p<0.05$ in all cases) during both memory encoding and
772 recall periods.
773
774 These results demonstrate that the reported directed information flow between different brain
775 areas during stimulation trials arise from causal signaling that is enhanced significantly above
776 chance levels.
777
778 *Effects of MTL stimulation on intra-regional information flow*
779
780 Next, we examined information flow between electrodes pairs within each of the individual brain
781 regions examine above. We found that information flow between the electrodes did not differ
782 between the stimulation and non-stimulation trials in any of the brain regions examined (MTL,
783 MFG, dorsal PPC, ventral PPC) during either memory encoding or recall in the delta-theta or
784 beta bands ($ps>0.05$, Cohen's $d < 1.16$). However, information flow in the IFG was higher for

785 stimulation, compared to non-stimulation, trials in the beta band during memory recall ($F(1, 60)$
786 $= 9.45$, $p<0.05$, Cohen's $d = 0.79$). These results indicate that MTL stimulation has minimal
787 effect on intra-regional directed information flow.
788
789 *Effects of MTL stimulation on phase synchronization between MTL and PFC and PPC*
790
791 In addition to analysis of time-delayed directed information flow using PTE, we also examined
792 instantaneous phase synchronization between the MTL and the PFC and PPC. Analysis of
793 instantaneous phase locking values (PLVs) (see **Methods**) revealed that phase locking of the
794 MTL with the MFG, IFG, dorsal PPC, ventral PPC did not differ between stimulation and non-
795 stimulation trials for either memory encoding or recall in the delta-theta or beta bands ($ps>0.05$,
796 Cohen's $d < 0.70$). These results suggest that the neuromodulatory effects of MTL stimulation
797 are a consequence of the time-delayed interactions between different brain areas as precisely
798 captured by the PTE measure rather than instantaneous synchronization measures such as the
799 PLV.
800
801 *Effects of MTL stimulation on intra-regional phase synchronization*
802
803 Next, we used PLV to examine information flow between electrodes pairs within each of the
804 individual brain regions. We found that phase locking between the electrodes did not differ
805 between stimulation and non-stimulation trials in any of the brain regions during both memory
806 encoding and recall, in the delta-theta or beta bands ($ps>0.05$, Cohen's $d < 0.42$). These results
807 indicate that MTL stimulation does not affect intra-region phase synchronization.

Effects of MTL stimulation on power in each individual brain region

We examined whether iEEG power differed between the stimulation and non-stimulation trials in each of the brain regions, as this may potentially underlie differences in directed information flow between the MTL and the PFC and PPC. We estimated power in the delta-theta and beta frequency bands (see **Methods**) for stimulation and non-stimulation trials and for both the memory encoding and recall periods. Power did not differ between stimulation and non-stimulation trials in the delta-theta or beta frequency bands in any of the brain regions (*ps*>0.05, Cohen's $d < 0.68$) (**Figure 6**).

Together, these results suggest that the differential directed information flow between the MTL and the PFC and PPC for stimulation and non-stimulation conditions are not driven by differences in the amplitude of iEEG fluctuations.

Effects of MTL stimulation on phase-amplitude coupling

Based on previous studies demonstrating phase-amplitude coupling (PAC) between low frequency delta-theta phase and amplitudes of high-gamma (80-160 Hz) frequency bands (Canolty et al., 2006; Tort et al., 2008), we examined the effects of stimulation on PAC in MTL, MFG, IFG, and dorsal and ventral PPC. We used the *modulation index* as an estimate of PAC in individual electrodes in different brain areas (Tort et al., 2008) (**Methods**). This analysis revealed that PAC did not differ between stimulation and non-stimulation trials in any of the

brain regions during memory encoding or recall (*ps*>0.05, Cohen's *d* <0.80). This suggests that stimulation of the MTL does not affect PAC in any of the five brain regions.

Discussion

We examined how MTL stimulation alters directed information flow between the MTL and frontoparietal cortical regions implicated in formation and monitoring of episodic memories. We used depth iEEG recordings from the UPENN-RAM cohort in which participants performed a verbal free recall task during concurrent stimulation of MTL neurons. During memory encoding, select MTL electrodes were electrically stimulated at 50 Hz on half the trials (Goyal et al., 2018; Jacobs et al., 2016). Building on our replicable prior findings of frequency specific interactions between the MTL and PFC (Das & Menon, 2021, 2022), we examined how MTL stimulation alters communication between the MTL and MFG subdivision of the PFC (i.e. dorsolateral PFC), during memory encoding, and how this stimulation altered communication during subsequent memory recall. MTL stimulation reduced memory recall (Cohen's effect size = 0.5) and disrupted directed information flow with the PFC. **Figure 7** summarizes our key findings.

MTL stimulation decreased MFG→MTL information flow in the delta-theta frequency band during the encoding period. Furthermore, the effects of MTL stimulation carried over from the encoding to the subsequent memory recall period, despite a ~20 sec delay period in which there was no external stimulation of the MTL. This process was characterized by decreased top-down MFG→MTL information flow in the beta frequency band. However, there was no difference in top-down PPC→MTL information flow. A direct comparison between the PFC and PPC revealed stronger modulation of top-down influences on the MTL from the PFC, compared to the PPC. Together, these findings demonstrate that MTL stimulation disrupts processing specifically

856 in the PFC in the low frequency delta-theta range during memory encoding with aftereffects that
857 extend to subsequent recall periods.
858
859 *MTL stimulation effects on directed MTL→PFC and PFC→MTL information flow during*
860 *memory encoding*
861
862 The primary goal of our study was to characterize the effect of MTL stimulation on directed
863 information flow between the MTL and the PFC during verbal episodic memory processing. The
864 MTL and MFG (dorsolateral PFC) play a critical role in human episodic memory encoding
865 (Anderson et al., 2010; Ekstrom & Watrous, 2014; Gonzalez et al., 2015; Neuner et al., 2014;
866 Watrous et al., 2013). However, it is unclear how electrical stimulation of the MTL modulates
867 neural dynamics of the targeted regions and the circuits that link them. Specifically, the effect of
868 stimulation on directed information flow between the MTL and the PFC during episodic memory
869 processing is poorly understood.
870
871 Our study builds on previously replicated findings across verbal episodic and spatial memory
872 domains which revealed higher bottom-up MTL→PFC information flow than the reverse, in
873 delta-theta and higher top-down PFC→MTL information flow than the reverse, in the beta
874 frequency bands (Das & Menon, 2021, 2022). We used phase transfer entropy (PTE), which
875 provides a robust and powerful tool for characterizing information flow between brain regions
876 based on phase coupling (Hillebrand et al., 2016; Lobier et al., 2014; M. Y. Wang et al., 2017).
877 We took an unbiased approach for assigning electrodes to individual anatomically-defined brain
878 regions and we did not select electrodes based on arbitrary task or stimulation-induced activation

879 profiles. Our approach thus allowed us to probe the electrophysiological correlates of the effects
880 of MTL stimulation on directed information flow between the MTL and PFC more generally.
881 We found that MTL stimulation decreased PFC→MTL information flow during the encoding
882 period, in delta-theta band. Notably, these effects were specific to the dorsolateral MFG
883 subdivision of the PFC and were not observed in the more ventral aspects that comprise the IFG.
884
885 We conducted control analyses to ensure that the reported effects related to the directed
886 information flow between the MTL and the MFG did not arise solely from brain stimulation
887 causing reorganization of brain circuits. Specifically, we used "resting-state" data from a
888 separate group of participants, also acquired and released as part of the UPENN-RAM public
889 data release (Solomon et al., 2021). Participants were instructed to sit quietly and did not perform
890 any task. Similar to the memory task, in the resting-state condition, bipolar stimulation current
891 between pairs of depth MTL electrodes was applied at 50 Hz. We found that, in contrast to the
892 memory task, neither MTL→MFG nor MFG→MTL directed information flow changed during
893 stimulation, compared to the non-stimulation, trials in the delta-theta frequency band. These
894 results suggest that directed information flow between the MTL and the MFG observed during
895 the memory task are not solely attributable to brain stimulation-induced reorganization of brain
896 circuits, rather they are related to the combined effects of stimulation and memory processing.
897
898 *MTL stimulation effects on directed MTL→PFC and PFC→MTL information flow during*
899 *memory recall*
900

Crucially, the effects of MTL stimulation were also detectable in the subsequent recall period which occurred after a delay of 20 seconds. This finding is consistent with previous human iEEG studies which have observed strong afterdischarge iEEG signals within and outside the MTL during memory retrieval, which occurred tens of seconds after MTL stimulation was applied during the encoding period of an episodic memory task (Halgren et al., 1985; Jun et al., 2020). Moreover, similar to our findings, these afterdischarge effects were linked to memory impairment in these studies (Halgren et al., 1985; Jun et al., 2020). Specifically, we observed decreased MFG→MTL information flow on stimulation, compared to non-stimulation, trials in the beta frequency band. Again, this effect was specific to the dorsolateral MFG subdivision of the PFC, which is known to play a prominent role in top-down control of both subcortical and cortical regions involved in memory formation (Brovelli et al., 2004; Engel & Fries, 2010; Spitzer & Haegens, 2017; Stanley, Roy, Aoi, Kopell, & Miller, 2018). Extending our findings of spectrally resolved top-down influences from the PFC, we found MTL stimulation effects in the beta-band but not in the delta-theta frequency band, providing consistent evidence for spectral dissociation associated with the beta frequency band. Theoretical models have pointed to both excitatory and inhibitory mechanisms underlying deep brain stimulation (McIntyre, Grill, Sherman, & Thakor, 2004; Vitek, 2002). We did not observe changes in power of iEEG signals in either frequency band, suggesting causal circuit mechanisms arising from phase, rather than amplitude, changes underlie the observed MTL stimulation related changes in information flow.

LFP studies in monkeys have demonstrated a more prominent role for the dorsal, compared to the ventral PFC, in top-down control in the beta frequency band for processing higher level abstractions during working memory performance (Wutz, Loonis, Roy, Donoghue, & Miller,

924 2018). Electrophysiology studies in rodents performing an odor-place associative memory
925 guided decision task on a T-maze have shown that hippocampal-PFC coherence in the beta
926 frequency band is linked to accurate decisions (Symanski, Bladon, Kullberg, Miller, & Jadhav,
927 2022). LFP studies in monkeys performing a paired association learning task have shown that
928 beta oscillations in the MFG encode picture-color association (Tanigawa et al., 2022). fMRI
929 studies in humans have shown that the dorsal MFG is a part of the central executive network
930 which plays an important role in memory processing and complex decision making (Menon &
931 Uddin, 2010; Seeley et al., 2007; Sridharan, Levitin, & Menon, 2008). Additionally,
932 magnetoencephalography and iEEG studies in humans have shown a prominent role of beta for
933 feedback signaling (Hayat et al., 2022; Michalareas et al., 2016). Consistent with our findings,
934 rodent studies have also shown that inhibition of PFC projections to the hippocampus impairs
935 memory recall (Rajasethupathy et al., 2015; Yadav et al., 2022). Reduction in neural signaling
936 from the MFG to the MTL during memory recall may explain why stimulation of the MTL
937 reduces or impairs memory performance (Coleshill et al., 2004; Goyal et al., 2018; Jacobs et al.,
938 2016; Lacruz et al., 2010).
939
940 A recent study using 1 Hz repetitive transcranial magnetic stimulation (rTMS) of the MFG found
941 enhancement of verbal memory performance and also showed that this stimulation induced
942 stronger beta power modulation in the posterior areas (van der Plas et al., 2021), suggesting that
943 neuromodulatory effects in the MFG might be the most prominent in the beta frequency band. A
944 meta-analysis of rTMS studies has revealed that 1 Hz rTMS of the MFG usually leads to an
945 enhancement of episodic memory performance, whereas 20 Hz rTMS of the MFG usually leads
946 to a reduction in episodic memory performance (Yeh & Rose, 2019). These results indicate a

947 disruptive effect of beta on MFG neural dynamics at frequencies significantly greater than 1 Hz,
948 including the 50 Hz stimulation frequency used in our study, and may explain the reduction of
949 information flow from the MFG that we observed during the recall periods in this frequency
950 band.
951
952 *Dissociable effects of MTL stimulation on top-down causal information flow from PFC and PPC*
953
954 The next goal of our study was to contrast the effects of MTL stimulation on information flow
955 with the PFC and PPC. In addition to the PFC, the PPC also plays an important role in episodic
956 memory (C. Moscovitch, Kapur, Köhler, & Houle, 1995; Schacter, Alpert, Savage, Rauch, &
957 Albert, 1996; Tulving et al., 1994). PTE analysis revealed that, in contrast to the PFC, there were
958 no differences between stimulation and non-stimulation trials in top-down dorsal PPC→MTL
959 information flow. A direct comparison revealed stronger MTL stimulation-induced modulation
960 of top-down MFG→MTL, compared to dorsal PPC→MTL in the beta frequency band (**Figure**
961 **4**). Information flow between the MTL and ventral PPC was unaffected by MTL stimulation, and
962 a direct comparison confirmed stronger MTL stimulation-induced modulation of top-down
963 MFG→MTL, compared to ventral PPC→MTL in the beta frequency band. This suggests that the
964 dorsolateral MFG subdivision of the PFC is more sensitive to MTL stimulation than PPC regions
965 involved in episodic memory.
966
967 Electrophysiology studies in monkeys have shown that the PFC is more sensitive to memory
968 encoding compared to the PPC (Dang, Li, Pu, Qi, & Constantinidis, 2022; Masse, Hodnefield, &
969 Freedman, 2017; Murray, Jaramillo, & Wang, 2017; Qi, Elworthy, Lambert, & Constantinidis,

2015; Zhou et al., 2021). Specifically, these studies showed that, compared to the PPC, neurons in the PFC are more responsive (Dang et al., 2022), show more persistent firing rate (Masse et al., 2017), and are more robust to distractors (Murray et al., 2017; Qi et al., 2015; Zhou et al., 2021). Together, these findings suggest that the MFG may play an enhanced role compared to the PPC in memory formation, which may make it a more sensitive target of brain stimulation compared to the PPC in humans (J. X. Wang et al., 2014).

Behavioral specificity of the effects of MTL stimulation

Finally, we examined whether the observed effects of MTL stimulation on information flow between different brain regions reflect cognitive processes related to memory encoding, or whether they are solely attributable to the reorganization of brain circuits from the effects of stimulation. We tested the hypothesis that the information flow between different brain areas would differ between successful and unsuccessful memory trials during stimulation, thus putatively reflecting cognitive processes related to memory processing, rather than effects of stimulation only.

We found that the direction of information flow between the MTL and both the PFC and PPC during memory recall is behaviorally relevant. Results support the hypotheses that causal signaling from the MTL to both regions are associated with memory recall processes, rather than arising solely from the effects of MTL stimulation-related reorganization of brain circuits. MTL→MFG directed information flow was significantly lower for successful, compared to

unsuccessful, memory recall in the beta band. This suggests that the higher causal signaling between the MTL→MFG in the beta band during unsuccessful trials is disruptive during recall.

Crucially, we found that the direction of information flow between the MTL and the ventral PPC during memory recall was also behaviorally relevant. MTL→vPPC directed information flow was significantly higher for successful, compared to unsuccessful, memory recall in both the delta-theta and beta frequency bands. MTL-vPPC have been previously proposed to form a coherent set of network and interactions within this network have been proposed to play a crucial role in memory processing in humans (Ranganath & Ritchey, 2012; Wagner et al., 2005). Moreover, non-invasive rTMS to the vPPC area is known to be associated with successful associative memory retrieval in humans (J. X. Wang et al., 2014). The increased MTL→vPPC directed information flow that we observed for the successful trials during memory recall is thus consistent with the prominent role of the vPPC for episodic memory retrieval and extends our understanding of directed causal signaling that supports such a role in the human brain.

Together, these results demonstrate that stimulating the MTL has a significant impact on communication between the MTL and the PFC and PPC, which can either enhance or hinder memory recall. Additionally, the results indicate that the direction of information flow in the MTL is not solely due to reorganization of brain circuits caused by stimulation, but rather a combination of stimulation and memory processing

Limitations

The stimulation paradigm used in the study was applied only at a single frequency (50 Hz) (**Methods**). Previous studies in humans have usually applied direct stimulation at theta and gamma frequencies to modulate memory performance, which are considered to be the endogenous rhythms of the MTL (Eichenbaum, 2017), although these frequencies have had a varied effect on memory performance. Whereas theta frequency stimulation have shown improvement in memory performance (Alagapan et al., 2019; Koubeissi, Kahriman, Syed, Miller, & Durand, 2013; Lee et al., 2013), stimulation at 50 Hz has shown heterogeneous patterns of memory performance, with some studies suggesting memory enhancement (Fell et al., 2013; Inman et al., 2018; Suthana et al., 2012), while others have found impairment in memory performance (Coleshill et al., 2004; Goyal et al., 2018; Jacobs et al., 2016; Lacruz et al., 2010). Limitations of electrode placement precluded analysis of causal circuit dynamics associated with each hemisphere and distinct subdivisions of the MTL; denser sampling of electrodes in multiple brain regions with a wider range of experimental tasks, and a larger number of participants are needed to further address these limitations. Additionally, studies with memory and resting-state iEEG data acquired in the same participants are needed to confirm that the effects of MTL stimulation reported in our study are not solely attributable to brain stimulation-induced reorganization of brain circuits. Finally, it is not known whether some of the patients may have shown considerable memory dysfunction in formal neuropsychological testing. Future studies with rigorous neuropsychological testing procedures are needed to determine the effect of brain stimulation in patients with different cognitive abilities.

In the present study, participants received stimulation at a range of current amplitudes, starting from 0.25 mA to 1.5 mA. The choice of the current amplitude values for the cognitive

experiments of the participants was the maximum current for each site that could be applied without inducing patient symptoms, epileptiform after discharges, or seizures. Lack of sufficient participants and electrode pairs for each of these current amplitude values did not allow us to study the effects of current amplitude on the information flow between the MTL and the PFC and PPC. Future studies will also need to consider the effects of a range of stimulation frequencies and currents, and electrode sites across MTL subdivisions in gray/white matter to rigorously assess other factors that influence memory performance, monitoring and directed information flow between the MTL and PFC.

Conclusions

Our findings provide novel evidence that MTL stimulation alters directed information flow with the PFC and PPC and that these influences are behaviorally relevant. Stimulating the MTL decreased flow of information from PFC to the MTL during both the encoding and recall periods, with effects lasting for more than 20 seconds after end of stimulation. This suppression of top-down PFC to MTL influences was stronger than suppression of PPC to MTL influences. Additionally, the flow of information from MTL to PFC was lower during successful memory recall compared to unsuccessful recall, while the flow of information from the MTL to the ventral PPC was higher during successful recall. These results show that the effects of MTL stimulation are specific to behavior, region, and direction, that MTL stimulation specifically impairs communication with the PFC, and that causal MTL-ventral PPC circuits support successful memory recall. Findings further suggest that information theoretic measures based on phase delays may provide a more robust measure of the effects of stimulation than other

measures such as changes in power and phase-amplitude coupling. Crucially, our findings demonstrate that suppression of the dorsolateral PFC is a locus of circuit vulnerability induced by MTL stimulation. Findings uncover a mechanism by which human MTL stimulation disrupts both formation and retrieval of recent memories (Halgren et al., 1985). Our findings have implications for translational applications aimed at realizing the promise of brain stimulation-based treatment of memory disorders.

References

Alagapan, S., Lustenberger, C., Hadar, E., Shin, H. W., & Fröhlich, F. (2019). Low-frequency direct cortical stimulation of left superior frontal gyrus enhances working memory performance. *Neuroimage, 184*, 697-706. doi:10.1016/j.neuroimage.2018.09.064

Amer, T., & Davachi, L. (2022). Neural Mechanisms of Memory. In M. J. Kahana & A. D. Wagner (Eds.), *Oxford Handbook of Human Memory*: Oxford University Press.

Amorapanth, P. X., Widick, P., & Chatterjee, A. (2010). The neural basis for spatial relations. *J Cogn Neurosci, 22*(8), 1739-1753. doi:10.1162/jocn.2009.21322

Andersen, R. A., Essick, G. K., & Siegel, R. M. (1985). Encoding of spatial location by posterior parietal neurons. *Science, 230*(4724), 456-458. doi:10.1126/science.4048942

Anderson, K. L., Rajagovindan, R., Ghacibeh, G. A., Meador, K. J., & Ding, M. (2010). Theta oscillations mediate interaction between prefrontal cortex and medial temporal lobe in human memory. *Cereb Cortex, 20*(7), 1604-1612. doi:10.1093/cercor/bhp223

Backus, A. R., Schoffelen, J. M., Szebényi, S., Hanslmayr, S., & Doeller, C. F. (2016). Hippocampal-Prefrontal Theta Oscillations Support Memory Integration. *Curr Biol, 26*(4), 450-457. doi:10.1016/j.cub.2015.12.048

Badre, D., Poldrack, R. A., Paré-Blagoev, E. J., Insler, R. Z., & Wagner, A. D. (2005). Dissociable controlled retrieval and generalized selection mechanisms in ventrolateral prefrontal cortex. *Neuron, 47*(6), 907-918. doi:10.1016/j.neuron.2005.07.023

Badre, D., & Wagner, A. D. (2007). Left ventrolateral prefrontal cortex and the cognitive control of memory. *Neuropsychologia, 45*(13), 2883-2901. doi:10.1016/j.neuropsychologia.2007.06.015

Barnett, L., & Seth, A. K. (2014). The MVGC multivariate Granger causality toolbox: A new approach to Granger-causal inference. *Journal of Neuroscience Methods, 223*, 50-68. doi:10.1016/j.jneumeth.2013.10.018

Baumann, O., Chan, E., & Mattingley, J. B. (2012). Distinct neural networks underlie encoding of categorical versus coordinate spatial relations during active navigation. *Neuroimage, 60*(3), 1630-1637. doi:10.1016/j.neuroimage.2012.01.089

Brincat, S. L., & Miller, E. K. (2015). Frequency-specific hippocampal-prefrontal interactions during associative learning. *Nat Neurosci, 18*(4), 576-581. doi:10.1038/nn.3954

Brovelli, A., Ding, M., Ledberg, A., Chen, Y., Nakamura, R., & Bressler, S. L. (2004). Beta oscillations in a large-scale sensorimotor cortical network: directional influences revealed by Granger causality. *Proc Natl Acad Sci U S A, 101*(26), 9849-9854. doi:10.1073/pnas.0308538101

Bruns, A. (2004). Fourier-, Hilbert- and wavelet-based signal analysis: are they really different approaches? *Journal of Neuroscience Methods, 137*(2), 321-332. doi:10.1016/j.jneumeth.2004.03.002

Buckner, R. L., Koutstaal, W., Schacter, D. L., Dale, A. M., Rotte, M., & Rosen, B. R. (1998). Functional-anatomic study of episodic retrieval. II. Selective averaging of event-related fMRI trials to test the retrieval success hypothesis. *Neuroimage, 7*(3), 163-175. doi:10.1006/nimg.1998.0328

Burke, J. F., Zaghloul, K. A., Jacobs, J., Williams, R. B., Sperling, M. R., Sharan, A. D., & Kahana, M. J. (2013). Synchronous and asynchronous theta and gamma activity during episodic memory formation. *J Neurosci, 33*(1), 292-304. doi:10.1523/jneurosci.2057-12.2013

1147 Cabeza, R. (2008). Role of parietal regions in episodic memory retrieval: the dual attentional
1148 processes hypothesis. *Neuropsychologia, 46*(7), 1813-1827.
1149 doi:10.1016/j.neuropsychologia.2008.03.019
1150 Cabeza, R., Ciaramelli, E., & Moscovitch, M. (2012). Cognitive contributions of the ventral
1151 parietal cortex: an integrative theoretical account. *Trends Cogn Sci, 16*(6), 338-352.
1152 doi:10.1016/j.tics.2012.04.008
1153 Cabeza, R., Ciaramelli, E., Olson, I. R., & Moscovitch, M. (2008). The parietal cortex and
1154 episodic memory: an attentional account. *Nat Rev Neurosci, 9*(8), 613-625.
1155 doi:10.1038/nrn2459
1156 Cabeza, R., Mazuz, Y. S., Stokes, J., Kragel, J. E., Woldorff, M. G., Ciaramelli, E., . . .
1157 Moscovitch, M. (2011). Overlapping parietal activity in memory and perception:
1158 evidence for the attention to memory model. *J Cogn Neurosci, 23*(11), 3209-3217.
1159 doi:10.1162/jocn_a_00065
1160 Canolty, R. T., Edwards, E., Dalal, S. S., Soltani, M., Nagarajan, S. S., Kirsch, H. E., . . . Knight,
1161 R. T. (2006). High gamma power is phase-locked to theta oscillations in human
1162 neocortex. *Science, 313*(5793), 1626-1628. doi:10.1126/science.1128115
1163 Chen, L. L., Lin, L. H., Green, E. J., Barnes, C. A., & McNaughton, B. L. (1994). Head-direction
1164 cells in the rat posterior cortex. I. Anatomical distribution and behavioral modulation.
1165 *Exp Brain Res, 101*(1), 8-23. doi:10.1007/bf00243212
1166 Chua, E. F., & Ahmed, R. (2016). Electrical stimulation of the dorsolateral prefrontal cortex
1167 improves memory monitoring. *Neuropsychologia, 85*, 74-79.
1168 doi:10.1016/j.neuropsychologia.2016.03.008
1169 Ciaramelli, E., Burianová, H., Vallesi, A., Cabeza, R., & Moscovitch, M. (2020). Functional
1170 Interplay Between Posterior Parietal Cortex and Hippocampus During Detection of
1171 Memory Targets and Non-targets. *Front Neurosci, 14*, 563768.
1172 doi:10.3389/fnins.2020.563768
1173 Ciaramelli, E., Grady, C. L., & Moscovitch, M. (2008). Top-down and bottom-up attention to
1174 memory: a hypothesis (AtoM) on the role of the posterior parietal cortex in memory
1175 retrieval. *Neuropsychologia, 46*(7), 1828-1851.
1176 doi:10.1016/j.neuropsychologia.2008.03.022
1177 Clower, D. M., West, R. A., Lynch, J. C., & Strick, P. L. (2001). The inferior parietal lobule is
1178 the target of output from the superior colliculus, hippocampus, and cerebellum. *J*
1179 *Neurosci, 21*(16), 6283-6291. doi:10.1523/jneurosci.21-16-06283.2001
1180 Coleshill, S. G., Binnie, C. D., Morris, R. G., Alarcón, G., van Emde Boas, W., Velis, D. N., . . .
1181 van Rijen, P. C. (2004). Material-specific recognition memory deficits elicited by
1182 unilateral hippocampal electrical stimulation. *J Neurosci, 24*(7), 1612-1616.
1183 doi:10.1523/jneurosci.4352-03.2004
1184 Crowe, D. A., Chafee, M. V., Averbeck, B. B., & Georgopoulos, A. P. (2004). Neural activity in
1185 primate parietal area 7a related to spatial analysis of visual mazes. *Cereb Cortex, 14*(1),
1186 23-34. doi:10.1093/cercor/bhg088
1187 Cruzado, N. A., Tiganj, Z., Brincat, S. L., Miller, E. K., & Howard, M. W. (2020). Conjunctive
1188 representation of what and when in monkey hippocampus and lateral prefrontal cortex
1189 during an associative memory task. *Hippocampus, 30*(12), 1332-1346.
1190 doi:10.1002/hipo.23282
1191 Curtis, C. E. (2006). Prefrontal and parietal contributions to spatial working memory.
1192 *Neuroscience, 139*(1), 173-180. doi:10.1016/j.neuroscience.2005.04.070

1193 Dang, W., Li, S., Pu, S., Qi, X. L., & Constantinidis, C. (2022). More Prominent Nonlinear
1194 Mixed Selectivity in the Dorsolateral Prefrontal than Posterior Parietal Cortex. *eNeuro,*
1195 *9*(2). doi:10.1523/eneuro.0517-21.2022
1196 Das, A., & Menon, V. (2020). Spatiotemporal Integrity and Spontaneous Nonlinear Dynamic
1197 Properties of the Salience Network Revealed by Human Intracranial Electrophysiology:
1198 A Multicohort Replication. *Cereb Cortex, 30*(10), 5309-5321.
1199 doi:10.1093/cercor/bhaa111
1200 Das, A., & Menon, V. (2021). Asymmetric frequency-specific feedforward and feedback
1201 information flow between hippocampus and prefrontal cortex during verbal memory
1202 encoding and recall. *Journal of Neuroscience*.
1203 Das, A., & Menon, V. (2022). Replicable patterns of causal information flow between
1204 hippocampus and prefrontal cortex during spatial navigation and spatial-verbal memory
1205 formation. *Cereb Cortex*. doi:10.1093/cercor/bhac018
1206 Daselaar, S. M., Prince, S. E., Dennis, N. A., Hayes, S. M., Kim, H., & Cabeza, R. (2009).
1207 Posterior midline and ventral parietal activity is associated with retrieval success and
1208 encoding failure. *Front Hum Neurosci, 3*, 13. doi:10.3389/neuro.09.013.2009
1209 Dickerson, B. C., & Eichenbaum, H. (2010). The episodic memory system: neurocircuitry and
1210 disorders. *Neuropsychopharmacology, 35*(1), 86-104.
1211 Dobbins, I. G., Foley, H., Schacter, D. L., & Wagner, A. D. (2002). Executive control during
1212 episodic retrieval: multiple prefrontal processes subserve source memory. *Neuron, 35*(5),
1213 989-996. doi:10.1016/s0896-6273(02)00858-9
1214 Eichenbaum, H. (2017). Prefrontal-hippocampal interactions in episodic memory. *Nat Rev*
1215 *Neurosci, 18*(9), 547-558. doi:10.1038/nrn.2017.74
1216 Ekstrom, A. D., Caplan, J. B., Ho, E., Shattuck, K., Fried, I., & Kahana, M. J. (2005). Human
1217 hippocampal theta activity during virtual navigation. *Hippocampus, 15*(7), 881-889.
1218 doi:10.1002/hipo.20109
1219 Ekstrom, A. D., & Watrous, A. J. (2014). Multifaceted roles for low-frequency oscillations in
1220 bottom-up and top-down processing during navigation and memory. *Neuroimage, 85 Pt*
1221 *2*, 667-677. doi:10.1016/j.neuroimage.2013.06.049
1222 Engel, A. K., & Fries, P. (2010). Beta-band oscillations--signalling the status quo? *Curr Opin*
1223 *Neurobiol, 20*(2), 156-165. doi:10.1016/j.conb.2010.02.015
1224 Ezzyat, Y., Wanda, P. A., Levy, D. F., Kadel, A., Aka, A., Pedisich, I., . . . Kahana, M. J. (2018).
1225 Closed-loop stimulation of temporal cortex rescues functional networks and improves
1226 memory. *Nat Commun, 9*(1), 365. doi:10.1038/s41467-017-02753-0
1227 Fan, L., Li, H., Zhuo, J., Zhang, Y., Wang, J., Chen, L., . . . Jiang, T. (2016). The Human
1228 Brainnetome Atlas: A New Brain Atlas Based on Connectional Architecture. *Cereb*
1229 *Cortex, 26*(8), 3508-3526. doi:10.1093/cercor/bhw157
1230 Fell, J., Staresina, B. P., Do Lam, A. T., Widman, G., Helmstaedter, C., Elger, C. E., &
1231 Axmacher, N. (2013). Memory modulation by weak synchronous deep brain stimulation:
1232 a pilot study. *Brain Stimul, 6*(3), 270-273. doi:10.1016/j.brs.2012.08.001
1233 Fernandez, G., Hufnagel, A., Helmstaedter, C., Zentner, J., & Elger, C. E. (1996). Memory
1234 function during low intensity hippocampal electrical stimulation in patients with temporal
1235 lobe epilepsy *European Journal of Neurology, 3*, 335-344.
1236 Gonzalez, A., Hutchinson, J. B., Uncapher, M. R., Chen, J., LaRocque, K. F., Foster, B. L., . . .
1237 Wagner, A. D. (2015). Electrocorticography reveals the temporal dynamics of posterior

parietal cortical activity during recognition memory decisions. *Proc Natl Acad Sci U S A, 112*(35), 11066-11071. doi:10.1073/pnas.1510749112

Goyal, A., Miller, J., Watrous, A. J., Lee, S. A., Coffey, T., Sperling, M. R., . . . Jacobs, J. (2018). Electrical Stimulation in Hippocampus and Entorhinal Cortex Impairs Spatial and Temporal Memory. *J Neurosci, 38*(19), 4471-4481. doi:10.1523/jneurosci.3049-17.2018

Grover, S., Nguyen, J. A., & Reinhart, R. M. G. (2021). Synchronizing Brain Rhythms to Improve Cognition. *Annu Rev Med, 72*, 29-43. doi:10.1146/annurev-med-060619-022857

Guitart-Masip, M., Barnes, G. R., Horner, A., Bauer, M., Dolan, R. J., & Duzel, E. (2013). Synchronization of medial temporal lobe and prefrontal rhythms in human decision making. *J Neurosci, 33*(2), 442-451. doi:10.1523/jneurosci.2573-12.2013

Gurd, J. M., Amunts, K., Weiss, P. H., Zafiris, O., Zilles, K., Marshall, J. C., & Fink, G. R. (2002). Posterior parietal cortex is implicated in continuous switching between verbal fluency tasks: an fMRI study with clinical implications. *Brain, 125*(Pt 5), 1024-1038. doi:10.1093/brain/awf093

Halgren, E., Wilson, C. L., & Stapleton, J. M. (1985). Human medial temporal-lobe stimulation disrupts both formation and retrieval of recent memories. *Brain Cogn, 4*(3), 287-295. doi:10.1016/0278-2626(85)90022-3

Hansen, N., Chaieb, L., Derner, M., Hampel, K. G., Elger, C. E., Surges, R., . . . Fell, J. (2018). Memory encoding-related anterior hippocampal potentials are modulated by deep brain stimulation of the entorhinal area. *Hippocampus, 28*(1), 12-17. doi:10.1002/hipo.22808

Hasegawa, I., Hayashi, T., & Miyashita, Y. (1999). Memory retrieval under the control of the prefrontal cortex. *Ann Med, 31*(6), 380-387. doi:10.3109/07853899908998795

Hayat, H., Marmelshtein, A., Krom, A. J., Sela, Y., Tankus, A., Strauss, I., . . . Nir, Y. (2022). Reduced neural feedback signaling despite robust neuron and gamma auditory responses during human sleep. *Nat Neurosci, 25*(7), 935-943. doi:10.1038/s41593-022-01107-4

Herweg, N. A., Solomon, E. A., & Kahana, M. J. (2020). Theta Oscillations in Human Memory. *Trends Cogn Sci, 24*(3), 208-227. doi:10.1016/j.tics.2019.12.006

Hillebrand, A., Tewarie, P., van Dellen, E., Yu, M., Carbo, E. W., Douw, L., . . . Stam, C. J. (2016). Direction of information flow in large-scale resting-state networks is frequency-dependent. *Proc Natl Acad Sci U S A, 113*(14), 3867-3872. doi:10.1073/pnas.1515657113

Huang, Y., & Keller, C. (2022). How can I investigate causal brain networks with iEEG? In N. Axmacher (Ed.), *Intracranial EEG for Cognitive Neuroscientists*: Springer.

Husain, M., & Nachev, P. (2007). Space and the parietal cortex. *Trends Cogn Sci, 11*(1), 30-36. doi:10.1016/j.tics.2006.10.011

Hutchinson, J. B., Uncapher, M. R., & Wagner, A. D. (2009). Posterior parietal cortex and episodic retrieval: convergent and divergent effects of attention and memory. *Learn Mem, 16*(6), 343-356. doi:10.1101/lm.919109

Inman, C. S., Manns, J. R., Bijanki, K. R., Bass, D. I., Hamann, S., Drane, D. L., . . . Willie, J. T. (2018). Direct electrical stimulation of the amygdala enhances declarative memory in humans. *Proc Natl Acad Sci U S A, 115*(1), 98-103. doi:10.1073/pnas.1714058114

Insausti, R., & Muñoz, M. (2001). Cortical projections of the non-entorhinal hippocampal formation in the cynomolgus monkey (Macaca fascicularis). *Eur J Neurosci, 14*(3), 435-451. doi:10.1046/j.0953-816x.2001.01662.x

1282 Jackson, J. B., Feredoes, E., Rich, A. N., Lindner, M., & Woolgar, A. (2021). Concurrent
1283 neuroimaging and neurostimulation reveals a causal role for dlPFC in coding of task-
1284 relevant information. *Commun Biol, 4*(1), 588. doi:10.1038/s42003-021-02109-x
1285 Jacobs, J., Miller, J., Lee, S. A., Coffey, T., Watrous, A. J., Sperling, M. R., . . . Rizzuto, D. S.
1286 (2016). Direct Electrical Stimulation of the Human Entorhinal Region and Hippocampus
1287 Impairs Memory. *Neuron, 92*(5), 983-990. doi:10.1016/j.neuron.2016.10.062
1288 Jun, S., Lee, S. A., Kim, J. S., Jeong, W., & Chung, C. K. (2020). Task-dependent effects of
1289 intracranial hippocampal stimulation on human memory and hippocampal theta power.
1290 *Brain Stimul, 13*(3), 603-613. doi:10.1016/j.brs.2020.01.013
1291 Kahana, M. J. (2006). The cognitive correlates of human brain oscillations. *J Neurosci, 26*(6),
1292 1669-1672. doi:10.1523/JNEUROSCI.3737-05c.2006
1293 Kim, K., Ekstrom, A. D., & Tandon, N. (2016). A network approach for modulating memory
1294 processes via direct and indirect brain stimulation: Toward a causal approach for the
1295 neural basis of memory. *Neurobiol Learn Mem, 134 Pt A*, 162-177.
1296 doi:10.1016/j.nlm.2016.04.001
1297 Konishi, S., Wheeler, M. E., Donaldson, D. I., & Buckner, R. L. (2000). Neural correlates of
1298 episodic retrieval success. *Neuroimage, 12*(3), 276-286. doi:10.1006/nimg.2000.0614
1299 Koubeissi, M. Z., Kahriman, E., Syed, T. U., Miller, J., & Durand, D. M. (2013). Low-frequency
1300 electrical stimulation of a fiber tract in temporal lobe epilepsy. *Ann Neurol, 74*(2), 223-
1301 231. doi:10.1002/ana.23915
1302 Kucewicz, M. T., Berry, B. M., Kremen, V., Miller, L. R., Khadjevand, F., Ezzyat, Y., . . .
1303 Worrell, G. A. (2018). Electrical Stimulation Modulates High γ Activity and Human
1304 Memory Performance. *eNeuro, 5*(1). doi:10.1523/eneuro.0369-17.2018
1305 Kucewicz, M. T., Berry, B. M., Miller, L. R., Khadjevand, F., Ezzyat, Y., Stein, J. M., . . .
1306 Worrell, G. A. (2018). Evidence for verbal memory enhancement with electrical brain
1307 stimulation in the lateral temporal cortex. *Brain, 141*(4), 971-978.
1308 doi:10.1093/brain/awx373
1309 Kucewicz, M. T., Cimbalnik, J., Matsumoto, J. Y., Brinkmann, B. H., Bower, M. R., Vasoli, V., .
1310 . . Worrell, G. A. (2014). High frequency oscillations are associated with cognitive
1311 processing in human recognition memory. *Brain, 137*(Pt 8), 2231-2244.
1312 doi:10.1093/brain/awu149
1313 Kumaran, D., Summerfield, J. J., Hassabis, D., & Maguire, E. A. (2009). Tracking the
1314 emergence of conceptual knowledge during human decision making. *Neuron, 63*(6), 889-
1315 901. doi:10.1016/j.neuron.2009.07.030
1316 Kuznetsova, A., Brockhoff, P. B., & Christensen, R. H. B. (2017). lmerTest Package: Tests in
1317 Linear Mixed Effects Models. *Journal of Statistical Software, 82*(13), 1-26.
1318 Kwon, H., Kronemer, S. I., Christison-Lagay, K. L., Khalaf, A., Li, J., Ding, J. Z., . . .
1319 Blumenfeld, H. (2021). Early cortical signals in visual stimulus detection. *Neuroimage,*
1320 *244*, 118608. doi:10.1016/j.neuroimage.2021.118608
1321 Lachaux, J. P., Axmacher, N., Mormann, F., Halgren, E., & Crone, N. E. (2012). High-frequency
1322 neural activity and human cognition: past, present and possible future of intracranial EEG
1323 research. *Prog Neurobiol, 98*(3), 279-301. doi:10.1016/j.pneurobio.2012.06.008
1324 Lachaux, J. P., Rodriguez, E., Martinerie, J., & Varela, F. J. (1999). Measuring phase synchrony
1325 in brain signals. *Hum Brain Mapp, 8*(4), 194-208. doi:10.1002/(sici)1097-
1326 0193(1999)8:4<194::aid-hbm4>3.0.co;2-c

1327 Lacruz, M. E., Valentín, A., Seoane, J. J., Morris, R. G., Selway, R. P., & Alarcón, G. (2010).
1328 Single pulse electrical stimulation of the hippocampus is sufficient to impair human
1329 episodic memory. *Neuroscience, 170*(2), 623-632.
1330 doi:10.1016/j.neuroscience.2010.06.042
1331 Lee, D. J., Gurkoff, G. G., Izadi, A., Berman, R. F., Ekstrom, A. D., Muizelaar, J. P., . . .
1332 Shahlaie, K. (2013). Medial septal nucleus theta frequency deep brain stimulation
1333 improves spatial working memory after traumatic brain injury. *J Neurotrauma, 30*(2),
1334 131-139. doi:10.1089/neu.2012.2646
1335 Lobier, M., Siebenhühner, F., Palva, S., & Matias, P. J. (2014). Phase transfer entropy: A novel
1336 phase-based measure for directed connectivity in networks coupled by oscillatory
1337 interactions. *Neuroimage, 85*, 853-872. doi:10.1016/j.neuroimage.2013.08.056
1338 Long, N. M., Burke, J. F., & Kahana, M. J. (2014). Subsequent memory effect in intracranial and
1339 scalp EEG. *Neuroimage, 84*, 488-494. doi:10.1016/j.neuroimage.2013.08.052
1340 Masse, N. Y., Hodnefield, J. M., & Freedman, D. J. (2017). Mnemonic Encoding and Cortical
1341 Organization in Parietal and Prefrontal Cortices. *J Neurosci, 37*(25), 6098-6112.
1342 doi:10.1523/jneurosci.3903-16.2017
1343 McIntyre, C. C., Grill, W. M., Sherman, D. L., & Thakor, N. V. (2004). Cellular effects of deep
1344 brain stimulation: model-based analysis of activation and inhibition. *J Neurophysiol,*
1345 *91*(4), 1457-1469. doi:10.1152/jn.00989.2003
1346 McNaughton, B. L., Mizumori, S. J., Barnes, C. A., Leonard, B. J., Marquis, M., & Green, E. J.
1347 (1994). Cortical representation of motion during unrestrained spatial navigation in the rat.
1348 *Cereb Cortex, 4*(1), 27-39. doi:10.1093/cercor/4.1.27
1349 Menon, V., Freeman, W. J., Cutillo, B. A., Desmond, J. E., Ward, M. F., Bressler, S. L., . . .
1350 Gevins, A. S. (1996). Spatio-temporal correlations in human gamma band
1351 electrocorticograms. *Electroencephalography and Clinical Neurophysiology, 98*(2), 89-
1352 102. doi:10.1016/0013-4694(95)00206-5
1353 Menon, V., & Uddin, L. Q. (2010). Saliency, switching, attention and control: a network model
1354 of insula function. *Brain Structure and Function, 214*(5), 655-667. doi:10.1007/s00429-
1355 010-0262-0
1356 Mercier, M. R., Dubarry, A. S., Tadel, F., Avanzini, P., Axmacher, N., Cellier, D., . . .
1357 Oostenveld, R. (2022). Advances in human intracranial electroencephalography research,
1358 guidelines and good practices. *Neuroimage*, 119438.
1359 doi:10.1016/j.neuroimage.2022.119438
1360 Merkow, M. B., Burke, J. F., Ramayya, A. G., Sharan, A. D., Sperling, M. R., & Kahana, M. J.
1361 (2017). Stimulation of the human medial temporal lobe between learning and recall
1362 selectively enhances forgetting. *Brain Stimul, 10*(3), 645-650.
1363 doi:10.1016/j.brs.2016.12.011
1364 Meyer-Lindenberg, A. S., Olsen, R. K., Kohn, P. D., Brown, T., Egan, M. F., Weinberger, D. R.,
1365 & Berman, K. F. (2005). Regionally specific disturbance of dorsolateral prefrontal-
1366 hippocampal functional connectivity in schizophrenia. *Arch Gen Psychiatry, 62*(4), 379-
1367 386. doi:10.1001/archpsyc.62.4.379
1368 Michalareas, G., Vezoli, J., van Pelt, S., Schoffelen, J. M., Kennedy, H., & Fries, P. (2016).
1369 Alpha-Beta and Gamma Rhythms Subserve Feedback and Feedforward Influences
1370 among Human Visual Cortical Areas. *Neuron, 89*(2), 384-397.
1371 doi:10.1016/j.neuron.2015.12.018

1372 Miyamoto, K., Osada, T., Adachi, Y., Matsui, T., Kimura, H. M., & Miyashita, Y. (2013).
1373 Functional differentiation of memory retrieval network in macaque posterior parietal
1374 cortex. *Neuron, 77*(4), 787-799. doi:10.1016/j.neuron.2012.12.019
1375 Mohan, U. R., Watrous, A. J., Miller, J. F., Lega, B. C., Sperling, M. R., Worrell, G. A., . . .
1376 Jacobs, J. (2020). The effects of direct brain stimulation in humans depend on frequency,
1377 amplitude, and white-matter proximity. *Brain Stimul, 13*(5), 1183-1195.
1378 doi:10.1016/j.brs.2020.05.009
1379 Moscovitch, C., Kapur, S., Köhler, S., & Houle, S. (1995). Distinct neural correlates of visual
1380 long-term memory for spatial location and object identity: a positron emission
1381 tomography study in humans. *Proc Natl Acad Sci U S A, 92*(9), 3721-3725.
1382 doi:10.1073/pnas.92.9.3721
1383 Moscovitch, M., Cabeza, R., Winocur, G., & Nadel, L. (2016). Episodic Memory and Beyond:
1384 The Hippocampus and Neocortex in Transformation. *Annu Rev Psychol, 67*, 105-134.
1385 doi:10.1146/annurev-psych-113011-143733
1386 Murray, J. D., Jaramillo, J., & Wang, X. J. (2017). Working Memory and Decision-Making in a
1387 Frontoparietal Circuit Model. *J Neurosci, 37*(50), 12167-12186.
1388 doi:10.1523/jneurosci.0343-17.2017
1389 Neuner, I., Arrubla, J., Werner, C. J., Hitz, K., Boers, F., Kawohl, W., & Shah, N. J. (2014). The
1390 default mode network and EEG regional spectral power: a simultaneous fMRI-EEG
1391 study. *PLoS One, 9*(2), e88214. doi:10.1371/journal.pone.0088214
1392 Nitz, D. A. (2006). Tracking route progression in the posterior parietal cortex. *Neuron, 49*(5),
1393 747-756. doi:10.1016/j.neuron.2006.01.037
1394 Paulk, A. C., Zelmann, R., Crocker, B., Widge, A. S., Dougherty, D. D., Eskandar, E. N., . . .
1395 Cash, S. S. (2022). Local and distant cortical responses to single pulse intracranial
1396 stimulation in the human brain are differentially modulated by specific stimulation
1397 parameters. *Brain Stimul, 15*(2), 491-508. doi:10.1016/j.brs.2022.02.017
1398 Peterson, R. A., & Cavanaugh, J. E. (2018). Ordered quantile normalization: a semiparametric
1399 transformation built for the cross-validation era. *Journal of Applied Statistics, 82*(13-15),
1400 2312–2327.
1401 Preston, A. R., & Eichenbaum, H. (2013). Interplay of hippocampus and prefrontal cortex in
1402 memory. *Curr Biol, 23*(17), R764-773. doi:10.1016/j.cub.2013.05.041
1403 Qi, X. L., Elworthy, A. C., Lambert, B. C., & Constantinidis, C. (2015). Representation of
1404 remembered stimuli and task information in the monkey dorsolateral prefrontal and
1405 posterior parietal cortex. *J Neurophysiol, 113*(1), 44-57. doi:10.1152/jn.00413.2014
1406 Qin, S., Cho, S., Chen, T., Rosenberg-Lee, M., Geary, D. C., & Menon, V. (2014).
1407 Hippocampal-neocortical functional reorganization underlies children's cognitive
1408 development. *Nat Neurosci, 17*(9), 1263-1269. doi:10.1038/nn.3788
1409 Rajasethupathy, P., Sankaran, S., Marshel, J. H., Kim, C. K., Ferenczi, E., Lee, S. Y., . . .
1410 Deisseroth, K. (2015). Projections from neocortex mediate top-down control of memory
1411 retrieval. *Nature, 526*(7575), 653-659. doi:10.1038/nature15389
1412 Ramirez-Zamora, A., Giordano, J., Gunduz, A., Alcantara, J., Cagle, J. N., Cernera, S., . . .
1413 Okun, M. S. (2020). Proceedings of the Seventh Annual Deep Brain Stimulation Think
1414 Tank: Advances in Neurophysiology, Adaptive DBS, Virtual Reality, Neuroethics and
1415 Technology. *Front Hum Neurosci, 14*, 54. doi:10.3389/fnhum.2020.00054
1416 Ranganath, C., & Ritchey, M. (2012). Two cortical systems for memory-guided behaviour. *Nat*
1417 *Rev Neurosci, 13*(10), 713-726. doi:10.1038/nrn3338

1418 Rockland, K. S., & Van Hoesen, G. W. (1999). Some temporal and parietal cortical connections
1419 converge in CA1 of the primate hippocampus. *Cereb Cortex, 9*(3), 232-237.
1420 doi:10.1093/cercor/9.3.232
1421 Rolls, E. T. (2018). The storage and recall of memories in the hippocampo-cortical system. *Cell*
1422 *Tissue Res, 373*(3), 577-604. doi:10.1007/s00441-017-2744-3
1423 Rolls, E. T. (2019). The cingulate cortex and limbic systems for action, emotion, and memory.
1424 *Handb Clin Neurol, 166*, 23-37. doi:10.1016/b978-0-444-64196-0.00002-9
1425 Rossini, P. M., & Rossi, S. (2007). Transcranial magnetic stimulation: diagnostic, therapeutic,
1426 and research potential. *Neurology, 68*(7), 484-488.
1427 doi:10.1212/01.wnl.0000250268.13789.b2
1428 Rugg, M. D. (2022). Frontoparietal Contributions to Retrieval. In M. J. Kahana & A. D. Wagner
1429 (Eds.), *Oxford Handbook of Human Memory*: Oxford University Press.
1430 Rugg, M. D., & Vilberg, K. L. (2013). Brain networks underlying episodic memory retrieval.
1431 *Curr Opin Neurobiol, 23*(2), 255-260. doi:10.1016/j.conb.2012.11.005
1432 Rutishauser, U., Reddy, L., Mormann, F., & Sarnthein, J. (2021). The Architecture of Human
1433 Memory: Insights from Human Single-Neuron Recordings. *J Neurosci, 41*(5), 883-890.
1434 doi:10.1523/jneurosci.1648-20.2020
1435 Schacter, D. L., Alpert, N. M., Savage, C. R., Rauch, S. L., & Albert, M. S. (1996). Conscious
1436 recollection and the human hippocampal formation: evidence from positron emission
1437 tomography. *Proc Natl Acad Sci U S A, 93*(1), 321-325. doi:10.1073/pnas.93.1.321
1438 Seeley, W. W., Menon, V., Schatzberg, A. F., Keller, J., Glover, G. H., Kenna, H., . . . Greicius,
1439 M. D. (2007). Dissociable Intrinsic Connectivity Networks for Salience Processing and
1440 Executive Control. *Journal of Neuroscience, 27*(9), 2349-2356.
1441 doi:10.1523/JNEUROSCI.5587-06.2007
1442 Simons, J. S., & Spiers, H. J. (2003). Prefrontal and medial temporal lobe interactions in long-
1443 term memory. *Nat Rev Neurosci, 4*(8), 637-648. doi:10.1038/nrn1178
1444 Solomon, E. A., Kragel, J. E., Sperling, M. R., Sharan, A., Worrell, G., Kucewicz, M., . . .
1445 Kahana, M. J. (2017). Widespread theta synchrony and high-frequency
1446 desynchronization underlies enhanced cognition. *Nature Communications, 8*(1), 1704.
1447 doi:10.1038/s41467-017-01763-2
1448 Solomon, E. A., Sperling, M. R., Sharan, A. D., Wanda, P. A., Levy, D. F., Lyalenko, A., . . .
1449 Kahana, M. J. (2021). Theta-burst stimulation entrains frequency-specific oscillatory
1450 responses. *Brain Stimul, 14*(5), 1271-1284. doi:10.1016/j.brs.2021.08.014
1451 Solomon, E. A., Stein, J. M., Das, S., Gorniak, R., Sperling, M. R., Worrell, G., . . . Kahana, M.
1452 J. (2019). Dynamic Theta Networks in the Human Medial Temporal Lobe Support
1453 Episodic Memory. *Curr Biol, 29*(7), 1100-1111.e1104. doi:10.1016/j.cub.2019.02.020
1454 Spaak, E., & de Lange, F. P. (2020). Hippocampal and Prefrontal Theta-Band Mechanisms
1455 Underpin Implicit Spatial Context Learning. *J Neurosci, 40*(1), 191-202.
1456 doi:10.1523/jneurosci.1660-19.2019
1457 Spitzer, B., & Haegens, S. (2017). Beyond the Status Quo: A Role for Beta Oscillations in
1458 Endogenous Content (Re)Activation. *eNeuro, 4*(4). doi:10.1523/eneuro.0170-17.2017
1459 Sridharan, D., Levitin, D. J., & Menon, V. (2008). A critical role for the right fronto-insular
1460 cortex in switching between central-executive and default-mode networks. *Proceedings*
1461 *of the National Academy of Sciences, 105*(34), 12569-12574.
1462 doi:10.1073/pnas.0800005105

1463 Stanley, D. A., Roy, J. E., Aoi, M. C., Kopell, N. J., & Miller, E. K. (2018). Low-Beta
1464 Oscillations Turn Up the Gain During Category Judgments. *Cereb Cortex, 28*(1), 116-
1465 130. doi:10.1093/cercor/bhw356
1466 Suthana, N., Haneef, Z., Stern, J., Mukamel, R., Behnke, E., Knowlton, B., & Fried, I. (2012).
1467 Memory enhancement and deep-brain stimulation of the entorhinal area. *N Engl J Med,*
1468 *366*(6), 502-510. doi:10.1056/NEJMoa1107212
1469 Symanski, C. A., Bladon, J. H., Kullberg, E. T., Miller, P., & Jadhav, S. P. (2022). Rhythmic
1470 coordination and ensemble dynamics in the hippocampal-prefrontal network during odor-
1471 place associative memory and decision making. *Elife, 11*. doi:10.7554/eLife.79545
1472 Tanigawa, H., Majima, K., Takei, R., Kawasaki, K., Sawahata, H., Nakahara, K., . . . Hasegawa,
1473 I. (2022). Decoding distributed oscillatory signals driven by memory and perception in
1474 the prefrontal cortex. *Cell Rep, 39*(2), 110676. doi:10.1016/j.celrep.2022.110676
1475 Tort, A. B., Kramer, M. A., Thorn, C., Gibson, D. J., Kubota, Y., Graybiel, A. M., & Kopell, N.
1476 J. (2008). Dynamic cross-frequency couplings of local field potential oscillations in rat
1477 striatum and hippocampus during performance of a T-maze task. *Proc Natl Acad Sci U S*
1478 *A, 105*(51), 20517-20522. doi:10.1073/pnas.0810524105
1479 Tulving, E., Kapur, S., Markowitsch, H. J., Craik, F. I., Habib, R., & Houle, S. (1994).
1480 Neuroanatomical correlates of retrieval in episodic memory: auditory sentence
1481 recognition. *Proc Natl Acad Sci U S A, 91*(6), 2012-2015. doi:10.1073/pnas.91.6.2012
1482 Uhlhaas, P. J., & Singer, W. (2012). Neuronal dynamics and neuropsychiatric disorders: toward
1483 a translational paradigm for dysfunctional large-scale networks. *Neuron, 75*(6), 963-980.
1484 doi:10.1016/j.neuron.2012.09.004
1485 Uncapher, M. R., & Wagner, A. D. (2009). Posterior parietal cortex and episodic encoding:
1486 insights from fMRI subsequent memory effects and dual-attention theory. *Neurobiol*
1487 *Learn Mem, 91*(2), 139-154. doi:10.1016/j.nlm.2008.10.011
1488 van der Plas, M., Braun, V., Stauch, B. J., & Hanslmayr, S. (2021). Stimulation of the left
1489 dorsolateral prefrontal cortex with slow rTMS enhances verbal memory formation. *PLoS*
1490 *Biol, 19*(9), e3001363. doi:10.1371/journal.pbio.3001363
1491 van Kesteren, M. T., Fernández, G., Norris, D. G., & Hermans, E. J. (2010). Persistent schema-
1492 dependent hippocampal-neocortical connectivity during memory encoding and
1493 postencoding rest in humans. *Proc Natl Acad Sci U S A, 107*(16), 7550-7555.
1494 doi:10.1073/pnas.0914892107
1495 Vincent, J. L., Snyder, A. Z., Fox, M. D., Shannon, B. J., Andrews, J. R., Raichle, M. E., &
1496 Buckner, R. L. (2006). Coherent spontaneous activity identifies a hippocampal-parietal
1497 memory network. *J Neurophysiol, 96*(6), 3517-3531. doi:10.1152/jn.00048.2006
1498 Vitek, J. L. (2002). Mechanisms of deep brain stimulation: excitation or inhibition. *Mov Disord,*
1499 *17 Suppl 3*, S69-72. doi:10.1002/mds.10144
1500 Vogt, B. A., & Pandya, D. N. (1987). Cingulate cortex of the rhesus monkey: II. Cortical
1501 afferents. *J Comp Neurol, 262*(2), 271-289. doi:10.1002/cne.902620208
1502 Wagner, A. D., Paré-Blagoev, E. J., Clark, J., & Poldrack, R. A. (2001). Recovering meaning:
1503 left prefrontal cortex guides controlled semantic retrieval. *Neuron, 31*(2), 329-338.
1504 doi:10.1016/s0896-6273(01)00359-2
1505 Wagner, A. D., Shannon, B. J., Kahn, I., & Buckner, R. L. (2005). Parietal lobe contributions to
1506 episodic memory retrieval. *Trends Cogn Sci, 9*(9), 445-453.
1507 doi:10.1016/j.tics.2005.07.001

Wang, J. X., Rogers, L. M., Gross, E. Z., Ryals, A. J., Dokucu, M. E., Brandstatt, K. L., . . . Voss, J. L. (2014). Targeted enhancement of cortical-hippocampal brain networks and associative memory. *Science, 345*(6200), 1054-1057. doi:10.1126/science.1252900

Wang, M. Y., Wang, J., Zhou, J., Guan, Y. G., Zhai, F., Liu, C. Q., . . . Luan, G. M. (2017). Identification of the epileptogenic zone of temporal lobe epilepsy from stereo-electroencephalography signals: A phase transfer entropy and graph theory approach. *Neuroimage Clin, 16*, 184-195. doi:10.1016/j.nicl.2017.07.022

Watrous, A. J., Tandon, N., Conner, C. R., Pieters, T., & Ekstrom, A. D. (2013). Frequency-specific network connectivity increases underlie accurate spatiotemporal memory retrieval. *Nature Neuroscience, 16*(3), 349-356. doi:10.1038/nn.3315

Wutz, A., Loonis, R., Roy, J. E., Donoghue, J. A., & Miller, E. K. (2018). Different Levels of Category Abstraction by Different Dynamics in Different Prefrontal Areas. *Neuron, 97*(3), 716-726.e718. doi:10.1016/j.neuron.2018.01.009

Yadav, N., Noble, C., Niemeyer, J. E., Terceros, A., Victor, J., Liston, C., & Rajasethupathy, P. (2022). Prefrontal feature representations drive memory recall. *Nature, 608*(7921), 153-160. doi:10.1038/s41586-022-04936-2

Yeh, N., & Rose, N. S. (2019). How Can Transcranial Magnetic Stimulation Be Used to Modulate Episodic Memory?: A Systematic Review and Meta-Analysis. *Front Psychol, 10*, 993. doi:10.3389/fpsyg.2019.00993

Zhang, W., Guo, L., & Liu, D. (2022). Concurrent interactions between prefrontal cortex and hippocampus during a spatial working memory task. *Brain Struct Funct, 227*(5), 1735-1755. doi:10.1007/s00429-022-02469-y

Zhou, Y., Rosen, M. C., Swaminathan, S. K., Masse, N. Y., Zhu, O., & Freedman, D. J. (2021). Distributed functions of prefrontal and parietal cortices during sequential categorical decisions. *Elife, 10*. doi:10.7554/eLife.58782

Figure captions

Figure 1. (a) Intracranial stimulation sites in the medial temporal lobe (MTL) investigated in this study. Each anode-cathode pair of electrodes is connected by a red line. MTL included the hippocampus, parahippocampal gyrus, and entorhinal cortex. **(b) Non-stimulation iEEG recording sites in the MTL, middle and inferior frontal gyrus subdivisions of the prefrontal cortex (MFG and IFG), and dorsal and ventral subdivisions of the posterior parietal cortex (dPPC and vPPC), investigated in this study. (c) Event structure of the verbal episodic memory task during non-stimulation (top panel) and stimulation (bottom panel) trials used in this study** (see **Methods** for details). Participants were first presented with a list of words in the encoding block and asked to recall as many as possible from the original list after a short delay (distractor period). Stimulation was provided in a blocked pattern; the stimulator was active during the presentation of a pair of consecutive words and then inactive for the following pair. On each stimulated list, the stimulator was active for half the total words (see **Methods** for details).

Figure 2. Directed information flow from PFC and PPC to the MTL in delta-theta band (0.5-8 Hz) during stimulation, compared to non-stimulation, trials in the memory encoding period. MFG → MTL information flow, measured using phase transfer entropy (PTE), was reduced during the stimulation, compared to non-stimulation, trials (n=132). In contrast, IFG→MTL (n=68), dorsal PPC→MTL (n=114), and ventral PPC→MTL (n=23) directed information flow did not differ between stimulation and non-stimulation trials. The central mark indicates the median, and the bottom and top edges of the box indicate the 25th and 75th percentiles, respectively. Whiskers extend to the most extreme data points not considered outliers. dPPC = dorsal PPC, vPPC = ventral PPC. ** $p < 0.01$ (FDR-corrected).

Figure 3. Directed information flow from the PFC and PPC to the MTL in beta band (12-30 Hz) during stimulation, compared to non-stimulation, trials in the memory recall period. MFG → MTL information flow was reduced during the stimulation trials compared to the non-stimulation trials (n=132). In contrast, IFG→MTL (n=68), dorsal PPC→MTL (n=114), and ventral PPC→MTL (n=23) directed information flow did not differ between stimulation and non-stimulation trials. dPPC = dorsal PPC, vPPC = ventral PPC. ** $p < 0.01$ (FDR-corrected).

Figure 4. Comparison of directed information flow from the MFG and dorsal/ventral PPC to the MTL in beta band (12-30 Hz) during stimulation trials in the memory recall period. MFG → MTL (n=132) information flow was significantly lower during the stimulation trials compared to both dorsal PPC→MTL (n=114) and ventral PPC→MTL (n=23) information flow. dPPC = dorsal PPC, vPPC = ventral PPC. *** $p < 0.001$, ** $p < 0.01$ (FDR-corrected).

Figure 5. Comparison of directed information flow from the MTL to the MFG and vPPC for successful compared to unsuccessful recall, during stimulation trials in the memory recall period. MTL → MFG (n=132) information flow was significantly reduced during successful, compared to unsuccessful, recall in the beta band. Moreover, MTL→ventral PPC (n=23) information flow was significantly higher during successful, compared to unsuccessful, recall in both the delta-theta and beta frequency bands. *** $p < 0.001$, ** $p < 0.01$ (FDR-corrected).

Figure 6. Spectral power in the delta-theta (0.5-8 Hz) and beta (12-30 Hz) frequency bands during stimulation compared to non-stimulation trials for the encoding and retrieval periods. (a) Spectral power in the delta-theta band during encoding periods. **(b)** Spectral power in the delta-theta band during recall periods. **(c)** Spectral power in the beta band during encoding periods. **(d)** Spectral power in the beta band during recall periods. Zero on the x-axis denotes the onset of word presentation for the encoding periods and the verbal recall of a word during the recall periods.

Figure 7. Schematic illustration of key findings related to MTL stimulation. (a) Directed information flow on successful trials. MTL stimulation decreased concurrent directed information flow from the middle frontal gyrus (MFG) subdivision of the prefrontal cortex to the MTL during memory encoding (delta-theta band). These effects were specific to MFG and were not observed in inferior frontal gyrus (IFG) or dorsal or ventral nodes of posterior parietal cortex. MTL stimulation aftereffects were observed in the subsequent memory recall period more than 20 seconds later, characterized by decreased top-down information flow from MFG to MTL (beta band); again, these effects were specific to MFG and were not observed in IFG or dorsal or ventral nodes of the posterior parietal cortex. Blue arrows show decrease during stimulation, compared to non-stimulation trials. **(b) Comparison of directed information flow during successful vs. unsuccessful memory recall.** MTL to MFG information flow on stimulation trials was significantly lower for successful, compared to unsuccessful, memory recall (beta band). In contrast, MTL to ventral posterior parietal cortex (PPC) information flow was significantly higher for successful, compared to unsuccessful, memory recall (both delta-theta and beta bands). Thickness of arrows correspond to relative strength of information flow, with higher thickness denoting stronger information flow.

Tables

Table 1. Participant demographic information for the memory task and stimulation details (total 14 participants).

Participant ID	Gender	Age	Stimulation electrode type (D= "depth")	Stimulation current amplitude
001	F	48	D	1 mA
003	F	39	D	1.5 mA
020	F	48	D	1.5 mA
030	M	23	D	1 mA
031	M	40	D	1.5 mA
033	F	31	D	1 mA
035	F	45	D	0.5 mA
056	M	34	D	1.5 mA
077	F	47	D	1 mA
085	F	30	D	1.5 mA
101	F	26	D	0.5 mA
111	M	20	D	0.75 mA
112	F	29	D	0.5 mA
150	F	49	D	0.25 mA

Table 2. Number of electrode pairs used in the phase transfer entropy (PTE) and phase locking value (PLV) analysis. MTL: medial temporal lobe; MFG: middle frontal gyrus, IFG: inferior frontal gyrus, dPPC: dorsal posterior parietal cortex; vPPC: ventral posterior parietal cortex.

Network pairs	Number of electrode pairs (n)	Number of participants	Participant IDs (Gender/Age)
MTL-MFG	132	4	003 (F/39), 020 (F/48), 033 (F/31), 077 (F/47)
MTL-IFG	68	5	003 (F/39), 020 (F/48), 035 (F/45), 077 (F/47), 101 (F/26)
MTL-dPPC	114	8	001 (F/48), 003 (F/39), 020 (F/48), 033 (F/31), 035 (F/45), 077 (F/47), 101 (F/26), 111 (M/20)
MTL-vPPC	23	4	033 (F/31), 077 (F/47), 101 (F/26), 111 (M/20)

Table 3. Number of electrodes in each brain region, used in power and phase-amplitude coupling analysis. MTL: medial temporal lobe; MFG: middle frontal gyrus, IFG: inferior frontal gyrus, dPPC: dorsal posterior parietal cortex; vPPC: ventral posterior parietal cortex.

Brain regions	Number of electrodes (n)	Number of participants	Participant IDs (Gender/Age)
MTL	30	10	001 (F/48), 003 (F/39), 020 (F/48), 031 (M/40), 033 (F/31), 035 (F/45), 077 (F/47), 101 (F/26), 111 (M/20), 112 (F/29)
MFG	51	7	003 (F/39), 020 (F/48), 030 (M/23), 033 (F/31), 056 (M/34), 077 (F/47), 085 (F/30)
IFG	35	9	003 (F/39), 020 (F/48), 030 (M/23), 035 (F/45), 056 (M/34), 077 (F/47), 085 (F/30), 101 (F/26), 150 (F/49)
dPPC	52	11	001 (F/48), 003 (F/39), 020 (F/48), 030 (M/23), 033 (F/31), 035 (F/45), 056 (M/34), 077 (F/47), 085 (F/30), 101 (F/26), 111 (M/20)
vPPC	9	4	033 (F/31), 077 (F/47), 101 (F/26), 111 (M/20)

Table 4. Differential effects of stimulation on directed information flow between the MTL and the MFG, IFG, dPPC, and vPPC. Results from 2-way ANOVA analysis with factors Region (MFG, IFG, dPPC, and vPPC) and Stimulation (ON/OFF). Statistically significant *p*-values of interaction, and main effects of Stimulation when interactions were non-significant, are indicated in bold (FDR-corrected for multiple comparisons).

Direction	Interaction effect (0.5-8 Hz)	Interaction effect (12-30 Hz)	Stimulation main effect (0.5-8 Hz)	Stimulation main effect (12-30 Hz)
Encode (MTL→PFC, PPC)	0.9138971	0.5496000	0.07382400	0.79940000
Encode (PFC, PPC→MTL)	**0.0025908**	0.5496000	0.00146600	0.41133333
Recall (MTL→PFC, PPC)	0.2090900	0.0482400	**0.02006667**	0.05436000
Recall (PFC, PPC→MTL)	0.9749598	**0.0025908**	0.42993429	0.00076512

Table 5. Differential effects of MTL stimulation on directed information flow for successful vs. unsuccessful memory during (a) Encoding and (b) Recall periods. Statistically significant *p*-values are indicated in bold (FDR-corrected for multiple comparisons).

(a) Memory Encoding

Direction	0.5-8 Hz	12-30 Hz
MTL→MFG	0.0252080	0.9950
MTL→IFG	0.9338286	0.9950
MTL→dPPC	0.0252080	0.9950
MTL→vPPC	0.9338286	0.9950
MFG→MTL	0.9338286	0.8712
IFG→MTL	0.9958000	0.9950
dPPC→MTL	0.9338286	0.9950
vPPC→MTL	0.9338286	0.9950

(b) Memory Recall

Direction	0.5-8 Hz	12-30 Hz
MTL→MFG	0.29573333	**0.00017304**
MTL→IFG	0.09964000	0.50540000
MTL→dPPC	0.44040000	0.04010667
MTL→vPPC	**0.00012136**	**0.00869200**
MFG→MTL	0.50053333	0.32848000
IFG→MTL	0.50053333	0.39906667
dPPC→MTL	0.68120000	0.32848000
vPPC→MTL	0.68120000	0.50540000

Table 6. Participant demographic information for analysis of resting-state iEEG (total 2 participants).

Participant ID	Gender	Age	Stimulation electrode type (D= "depth")	Stimulation current amplitude	Stimulation duration
054	M	23	D	1 mA	250 ms
136	F	56	D	2 mA	500 ms

a

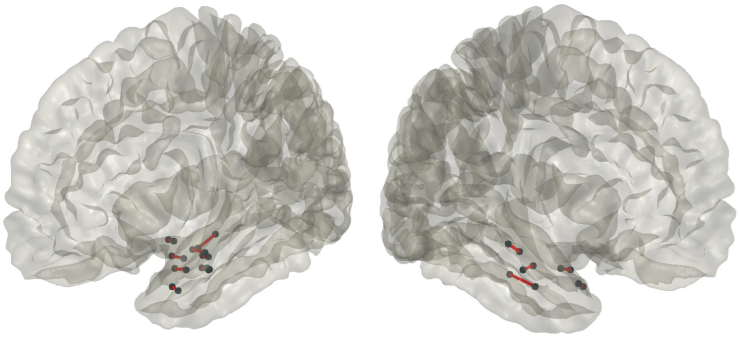

b

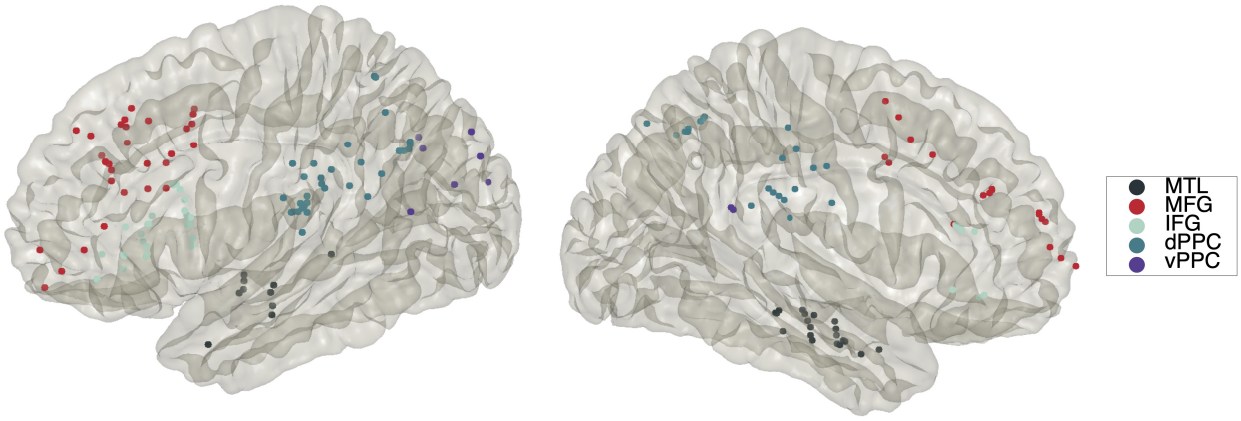

c

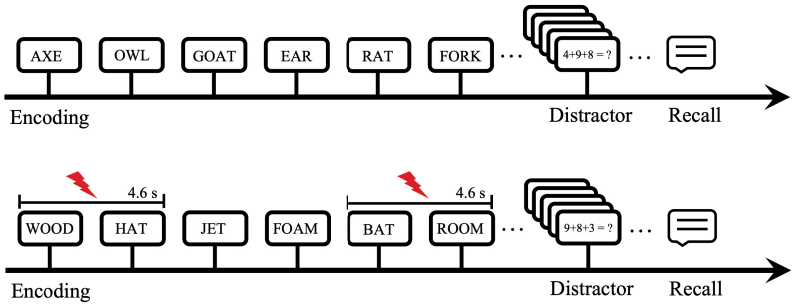

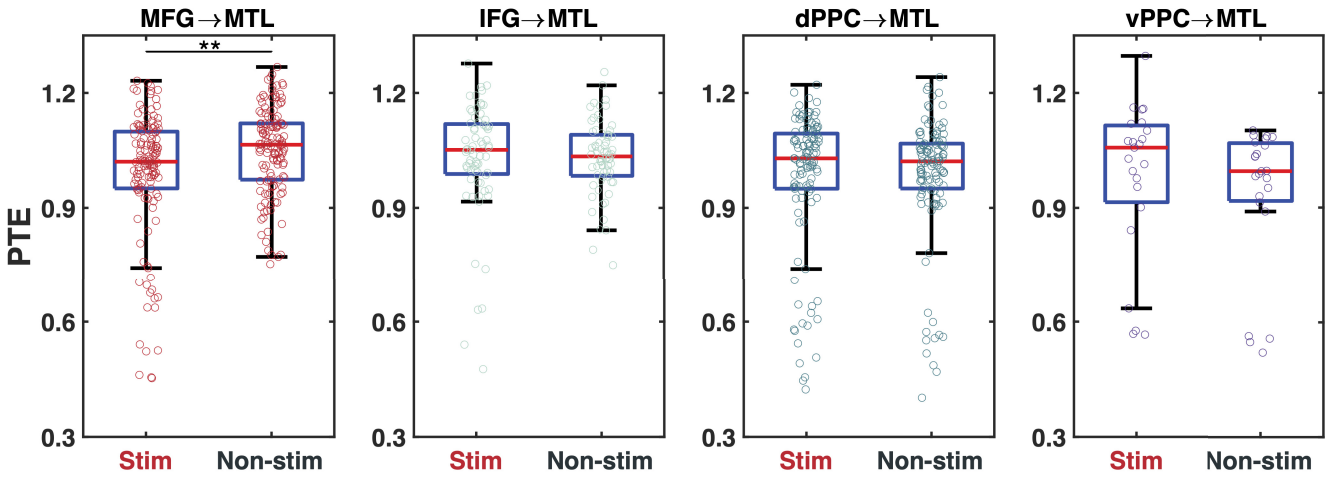

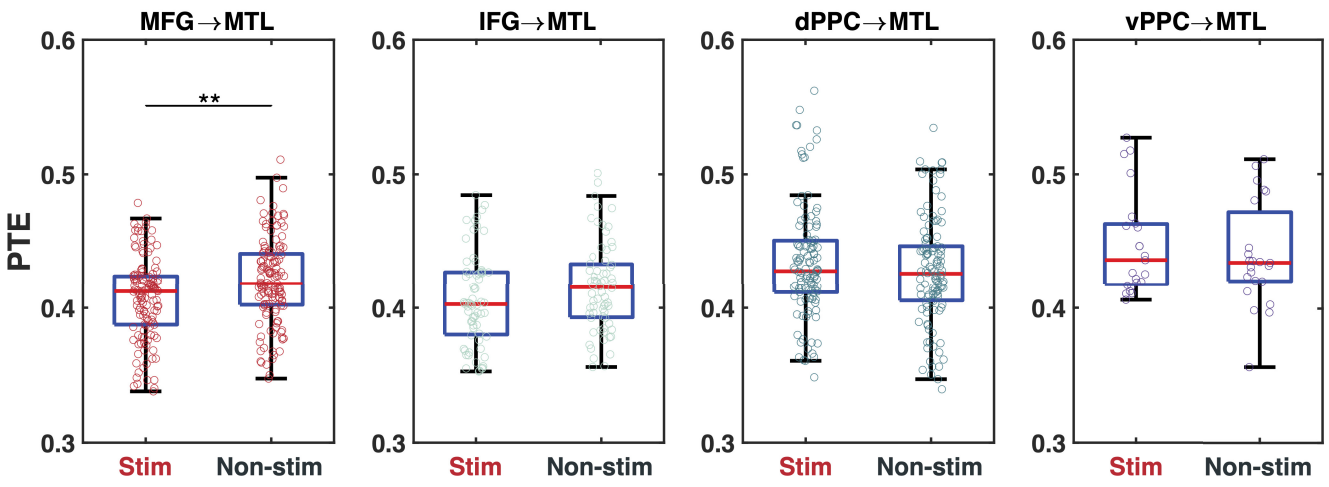

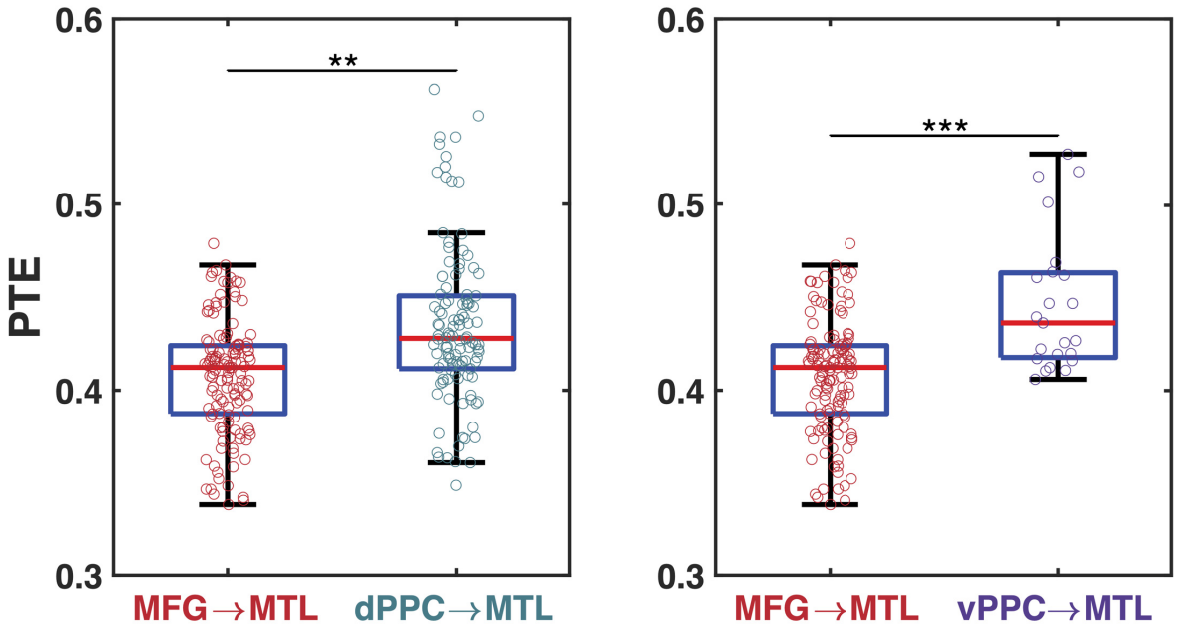

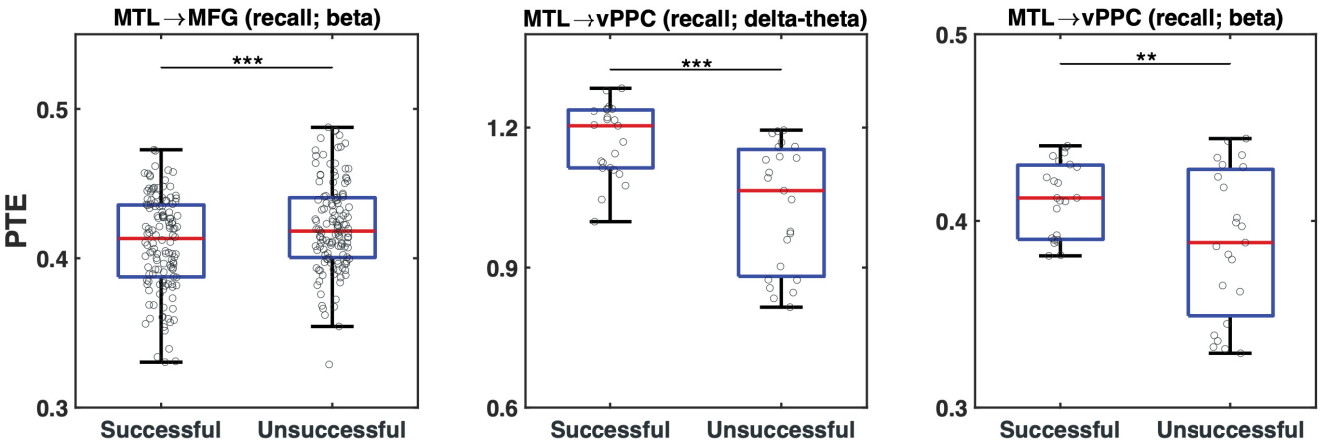

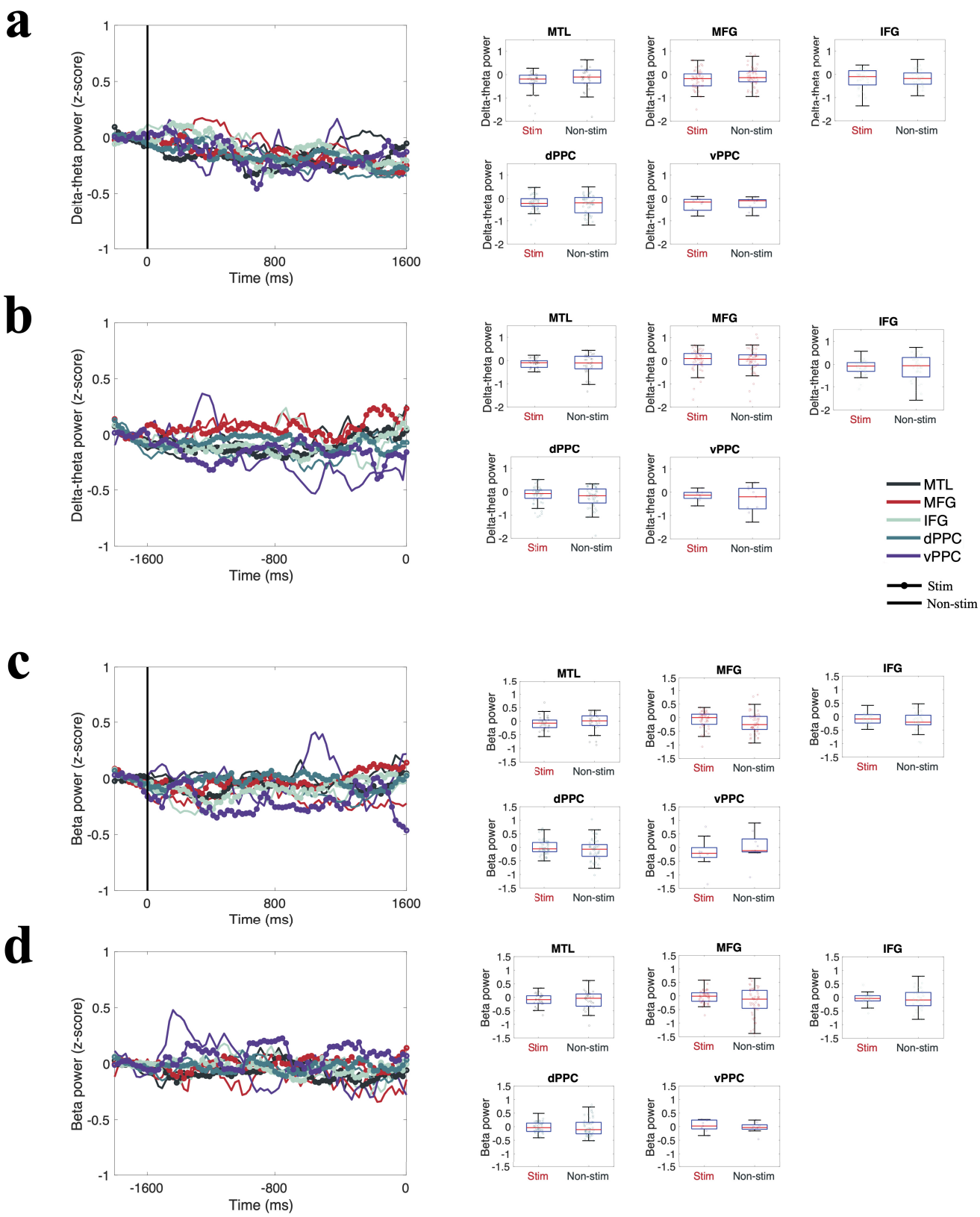

a

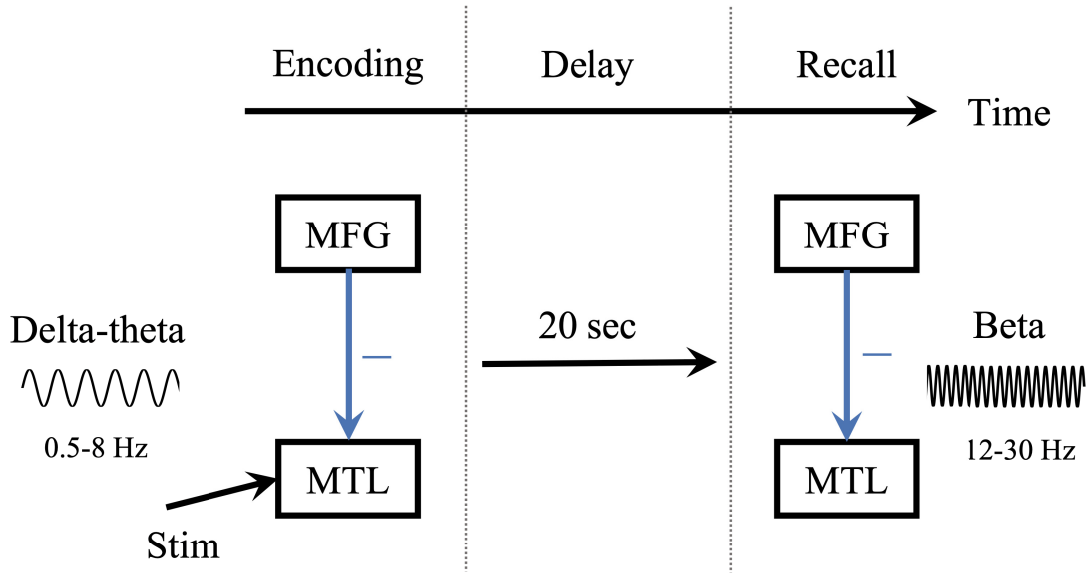

b